Supplementary information

Garciyunnanimines A-C, novel cytotoxic polycyclic polyprenylated acylphloroglucinol imines from *Garcinia yunnanensis*

Dan Zheng,[a,†] Hong Zhang,[a,†] Chang-Wu Zheng,[a,b] Yuan-Zhi Lao,[a] Dan-Qing Xu,[a] Lian-Bo Xiao,[c] and Hong-Xi Xu [a,c]

[a] School of Pharmacy, Shanghai University of Traditional Chinese Medicine, Shanghai 201203, China. E-mail: xuhongxi88@gmail.com (H.-X. Xu)

[b] Key Laboratory of Synthetic Chemistry of Natural Substances, Shanghai Institute of Organic Chemistry, Chinese Academy of Sciences, Shanghai 200032, China.

[c] Institute of Arthritis Research, Shanghai Academy of Chinese Medical Sciences, Guanghua Integrative Medicine Hospital, Shanghai 201203, China. E-mail: 13701888178@163.com (L.-B. Xiao)

[†] These authors contributed equally to this work.

List of Supplementary Information

Part 1 Experimental Section

Part 2 Results and HRESIMS, IR, ECD, and NMR spectra of compounds 1–5

Supplementary information Available

Part 1. Experimental section

1. Analysis of compounds **1** and **3** in a new plant extract by UPLC-ESI-QTOF-MS

1.1 Sample preparation

The Air-dried power of *G. garciyunnanensis* (108 g, with the same origin that the plant material used for the initial extraction) were extracted by hot reflux with 95% EtOH (3 × 1 L, each 1h). The crude extract was suspended in H_2O and partitioned by petroleum ether-soluble, EtOAc, respectively. And then The petroleum ether-soluble portion was subjected to passage over a chromatography column (CC) on MCI, and successively eluted with H_2O and 95% EtOH. The 95% EtOH-eluting fraction was evaporated to dryness under vacuum and was chromatographed by reversed-phase C_{18} silica gel CC. The column was eluted in a step-gradient manner with MeOH-H_2O (30%→100%), and each 200 mL of the eluate was collected as one fraction. Finally, 29 fractions (Fr.1-29) were obtained. After filtration through 0.22 μm microporous membrane, 2 μL of each sample was injected for UPLC-ESI-QTOF-MS analysis.

2.2 UPLC-ESI-QTOF-MS analysis

UPLC analysis was performed on a Waters ACQUITY UPLC TM system (Waters corporation, Milford, MA, USA), equipped with a binary solvent delivery system and an autosampler. Samples were eluted on a Waters ACQUITY BEH C_{18} column (100 mm × 2.1 mm, 1.7 μm). The column was maintained at 40 °C. A mobile phase consisting of 0.1% formic acid in water (A) and CH_3CN (B) was applied with the optimized gradient program as follows: 32%−42% B (0−5 min), 42%−46% B (5−10 min), 46%−70% B (10−23 min), 70−95% B (23−29 min), 95-100% B (29-32 min), 100%−95% B (32−33 min), 95%−32% B (33−35 min), and 32% B (35-40 min). The flow rate was kept at 0.4 mL/min. The sample volume injected was set at 2 μL.

Mass spectrometry was performed on a Waters Q-TOF Synapt G2-Si mass spectrometer (Waters MS Technologies, Manchester, UK) equipped with electrospray ionization (ESI) source operating in negative mode. The desolvation gas flow rate was 800 L/h at a temperature of 400 °C. The cone gas was 50 L/h. The source temperature was 100 °C. The capillary voltage and cone voltage were set at 3000 V and 40 V, respectively. The instrument was calibrated with sodium formate. The mass accuracy and reproducibility were maintained using a LockSpray^{TM} and the $[M + H]^-$ ion of 159 leucine-enkephalin infused at 5 μL/min was used as a reference lock mass (*m/z* 556.2771 Da) at the concentration of 1 ng/μL. Centroided data were acquired for each sample from 50 to 1200 Da.

2. Computational details

The theoretical calculations of compounds **1**−**5** were performed using Gaussian 09.[1] Conformational analysis was initially carried out using Accelrys Discovery Studio 2.5 to generate conformations by Best, then minimize them by Smart Minimizer using the CHARMm molecular mechanics force field. The minimized conformers were further optimized at the B3LYP/6-31G (d, g) level in the gas phase. Room-temperature equilibrium populations were calculated according to the Boltzmann distribution law. The theoretical calculation of ECD was performed using TDDFT at the B3LYP/6-31G (d, p) level in the gas phase. The ECD spectra of **1**−**5** were obtained by weighing the Boltzmann distribution rate of each geometric conformation. SpecDis 1.61[2] was used to sum up single CD spectra after a Boltzmann statistical weighting, for the gauss curve generation and for the comparison with experimental data.

References:

(1) Gaussian 09, Revision D.01, M. J. Frisch, G. W. Trucks, H. B. Schlegel, G. E. Scuseria, M. A. Robb, J. R.

Cheeseman, G. Scalmani, V. Barone, B. Mennucci, G. A. Petersson, H. Nakatsuji, M. Caricato, X. Li, H. P. Hratchian, A. F. Izmaylov, J. Bloino, G. Zheng, J. L. Sonnenberg, M. Hada, M. Ehara, K. Toyota, R. Fukuda, J. Hasegawa, M. Ishida, T. Nakajima, Y. Honda, O. Kitao, H. Nakai, T. Vreven, J. A. Montgomery, Jr., J. E. Peralta, F. Ogliaro, M. Bearpark, J. J. Heyd, E. Brothers, K. N. Kudin, V. N. Staroverov, T. Keith, R. Kobayashi, J. Normand, K. Raghavachari, A. Rendell, J. C. Burant, S. S. Iyengar, J. Tomasi, M. Cossi, N. Rega, J. M. Millam, M. Klene, J. E. Knox, J. B. Cross, V. Bakken, C. Adamo, J. Jaramillo, R. Gomperts, R. E. Stratmann, O. Yazyev, A. J. Austin, R. Cammi, C. Pomelli, J. W. Ochterski, R. L. Martin, K. Morokuma, V. G. Zakrzewski, G. A. Voth, P. Salvador, J. J. Dannenberg, S. Dapprich, A. D. Daniels, O. Farkas, J. B. Foresman, J. V. Ortiz, J. Cioslowski, and D. J. Fox, Gaussian, Inc., Wallingford CT, 2013.

(2) T. Bruhn, A. Schaumlöffel, Y. Hemberger, G. Bringmann, SpecDis version 1.64, University of Wuerzburg, Germany, 2015.

Part 2 Results and HRESIMS, IR, ECD, and NMR spectra of compounds **1**–**5**

Table S1. Survey of reaction conditions for **2**

entry	ammonia (equiv.)	acetic acid (equiv.)	temperature (℃)	time (h)	yield (%)
1	10[a]	0	room temperature	2	0
2	10[a]	0	80	2	0
4	2[b]	0	80	4	3
5	10[b]	100	80	2	12
7	50[b]	100	80	2	47
8	50[b]	1000	80	2	55
9	200[b]	1000	80	4	69
10	200[b]	1000	room temperature	4	9
11	200[b]	1000	room temperature	24	10
12	400[b]	1000	80	4	60
13	200[b]	1000	100	4	52
14	200[c]	1000	80	4	47

[a] ammonia water, compound was dissolved in MeOH
[b] ammonia (0.5M in dioxane)
[c] ammonia (7M in MeOH)

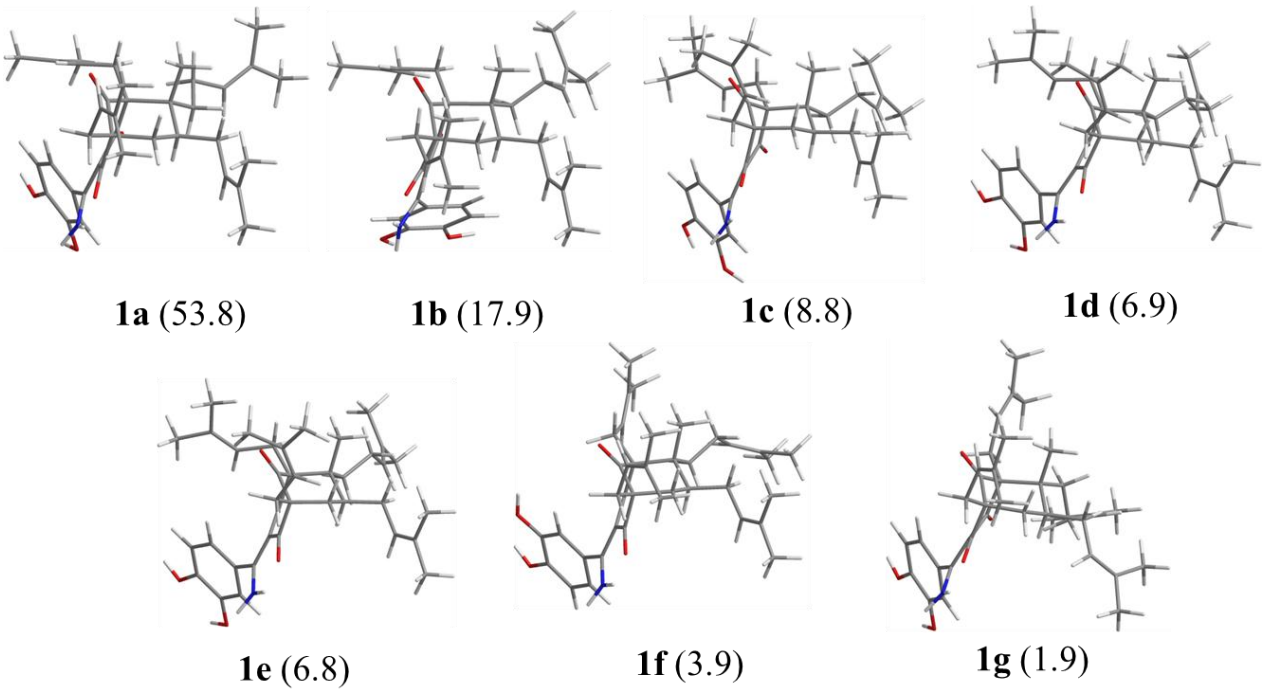

Figure CS1. The stable conformers of (1*S*,5*R*,6*R*,7*S*)-**1** calculated with DFT at the B3LYP/6-31G (d, g) level. Relative populations are in parentheses. Equilibrium Populations calculated by the relative free Gibbs energies at B3LYP/6-31G (d) level in the gas phase, assuming Boltzman statistics at T = 298.15 K and 1 atm.

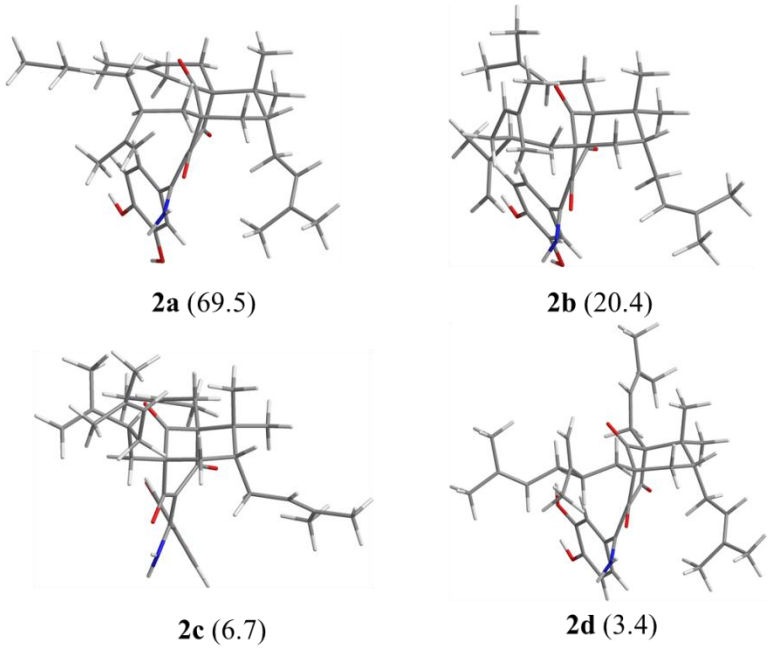

Figure CS2. The stable conformers of (1*R*,5*R*,7*R*,30*S*)-**2** calculated with DFT at the B3LYP/6-31G (d, g) level. Relative populations are in parentheses. Equilibrium Populations calculated by the relative free Gibbs energies at B3LYP/6-31G (d) level in the gas phase, assuming Boltzman statistics at T = 298.15 K and 1 atm.

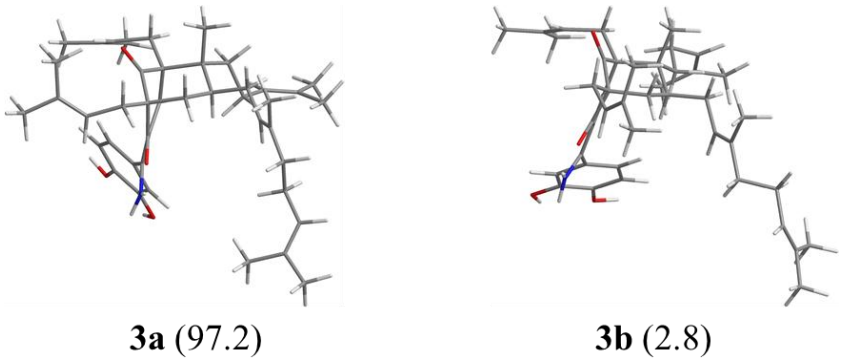

Figure CS3. The stable conformers of (1*R*,5*R*,6*R*,7*S*)-**3** calculated with DFT at the B3LYP/6-31G (d, g) level. Relative populations are in parentheses. Equilibrium Populations calculated by the relative free Gibbs energies at B3LYP/6-31G (d) level in the gas phase, assuming Boltzman statistics at T = 298.15 K and 1 atm.

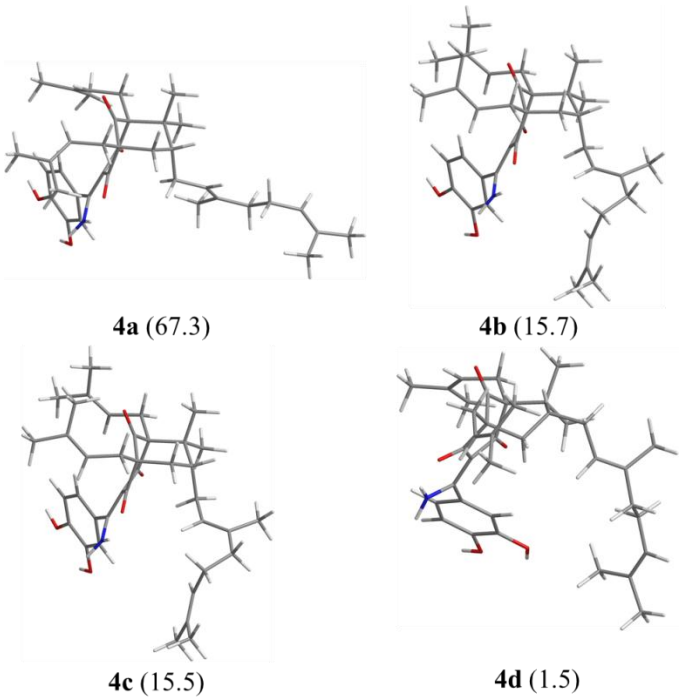

Figure CS4. The stable conformers of (1*S*,5*R*,6*R*,7*S*)-**4** calculated with DFT at the B3LYP/6-31G (d, g) level. Relative populations are in parentheses. Equilibrium Populations calculated by the relative free Gibbs energies at B3LYP/6-31G (d) level in the gas phase, assuming Boltzman statistics at T = 298.15 K and 1 atm.

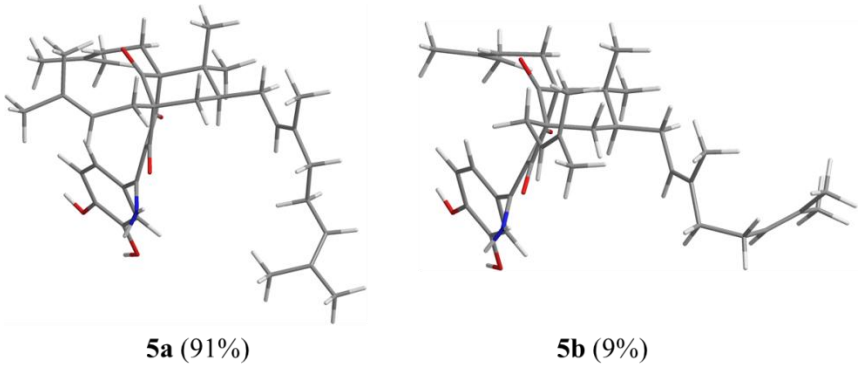

Figure CS5. The stable conformers of (1*S*,5*R*,6*R*,7*R*)-**5** calculated with DFT at the B3LYP/6-31G (d, g) level. Relative populations are in parentheses. Equilibrium Populations calculated by the relative free Gibbs energies at B3LYP/6-31G (d) level in the gas phase, assuming Boltzman statistics at T = 298.15 K and 1 atm.

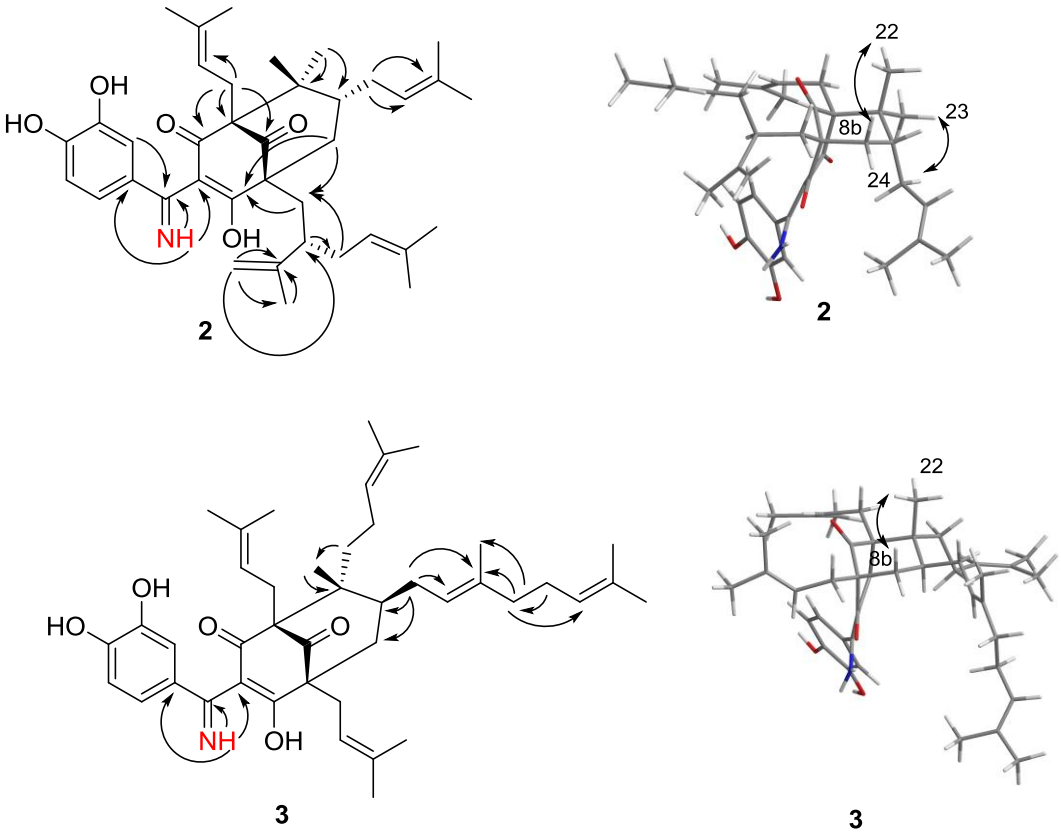

Figure S1. Key correlations observed in the HMBC and NOESY NMR spectra of **2** and **3**.

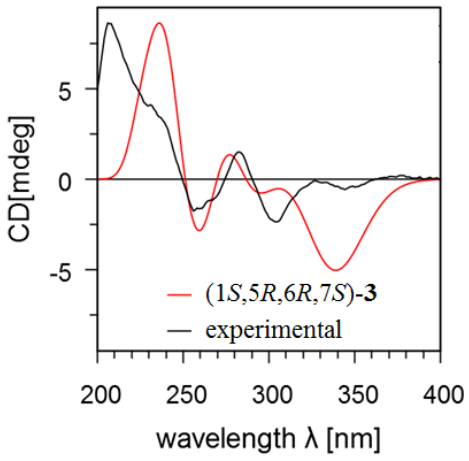

Figure S2. Calculated ECD spectrum of **3** its experimental curv

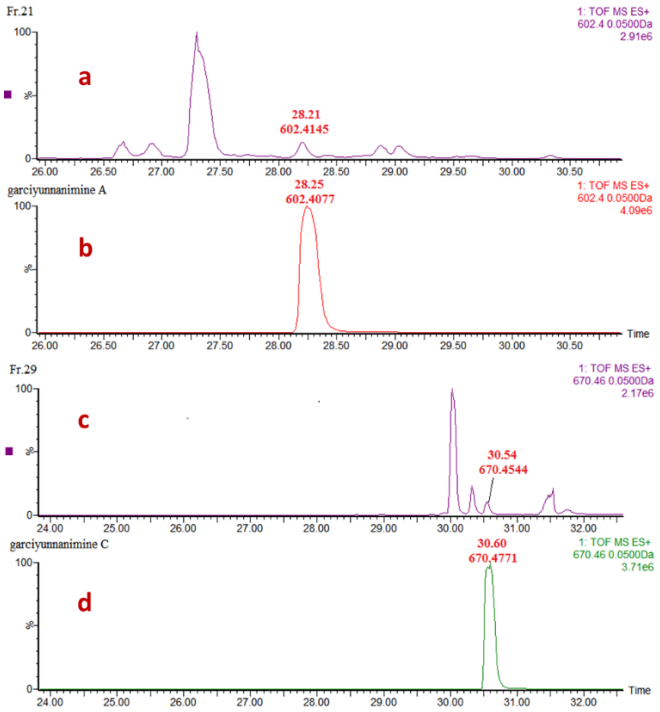

Figure S3. UPLC-ESI-QTOF-MS analysis of compounds **1** and **3** in a new plant extract of *G. yunnanensis*. (a) the extracted ion chromatogram (EIC) of Fr. 21 (ions at m/z 602.38), (b) the extracted ion chromatogram (EIC) of compound **1** (ions at m/z 602.38), (c) EIC of Fr. 29 (ions at m/z 670.46), (d) EIC of compound **3** (ions at m/z 670.46)

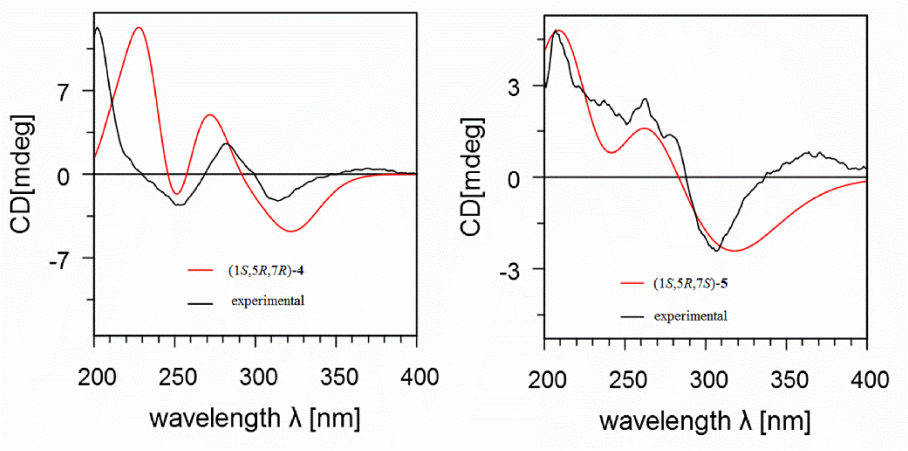

Figure S4. Calculated ECD spectra of **4** and **5** and its experimental curves.

Garciyunnanimine A (**1**)

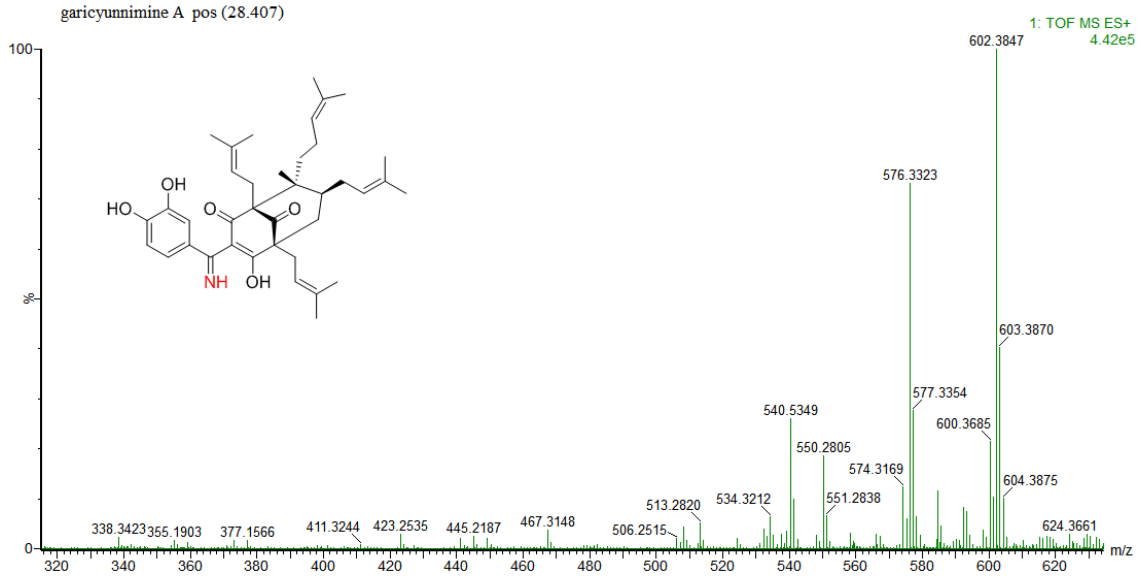

Figure S5. HRESIMS spectrum of **1**

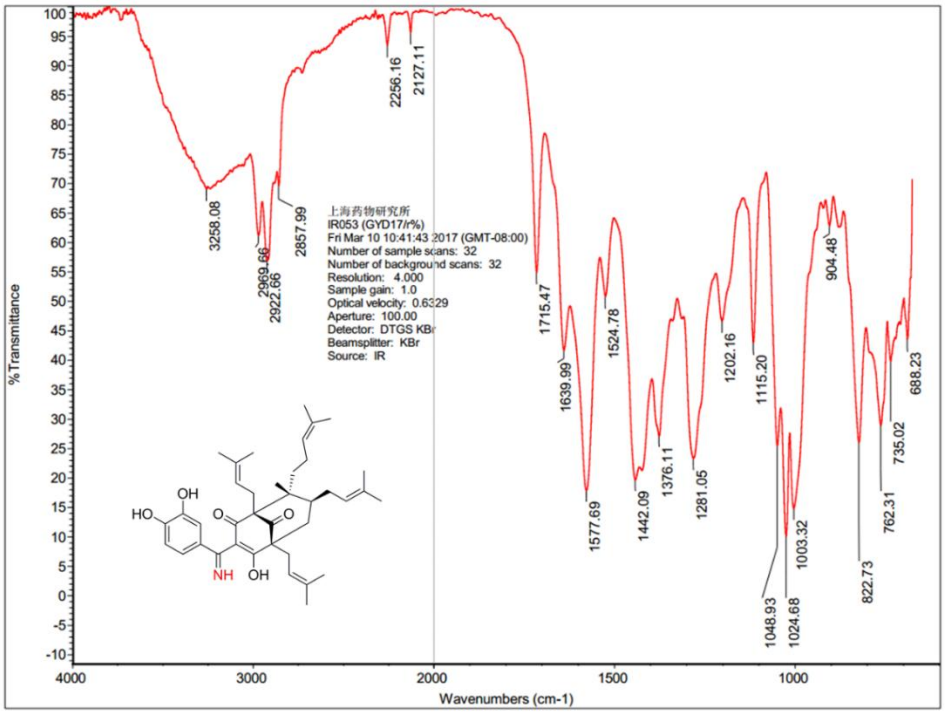

Figure S6. IR (KBr, disc) spectrum of **1**

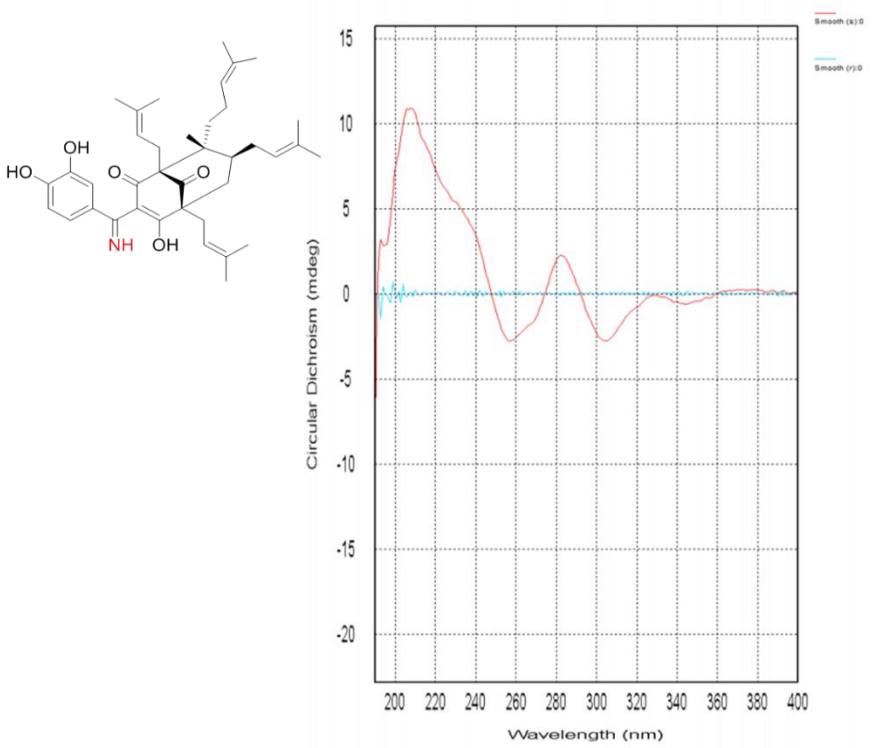

Figure S7. Experimental ECD spectrum of **1**

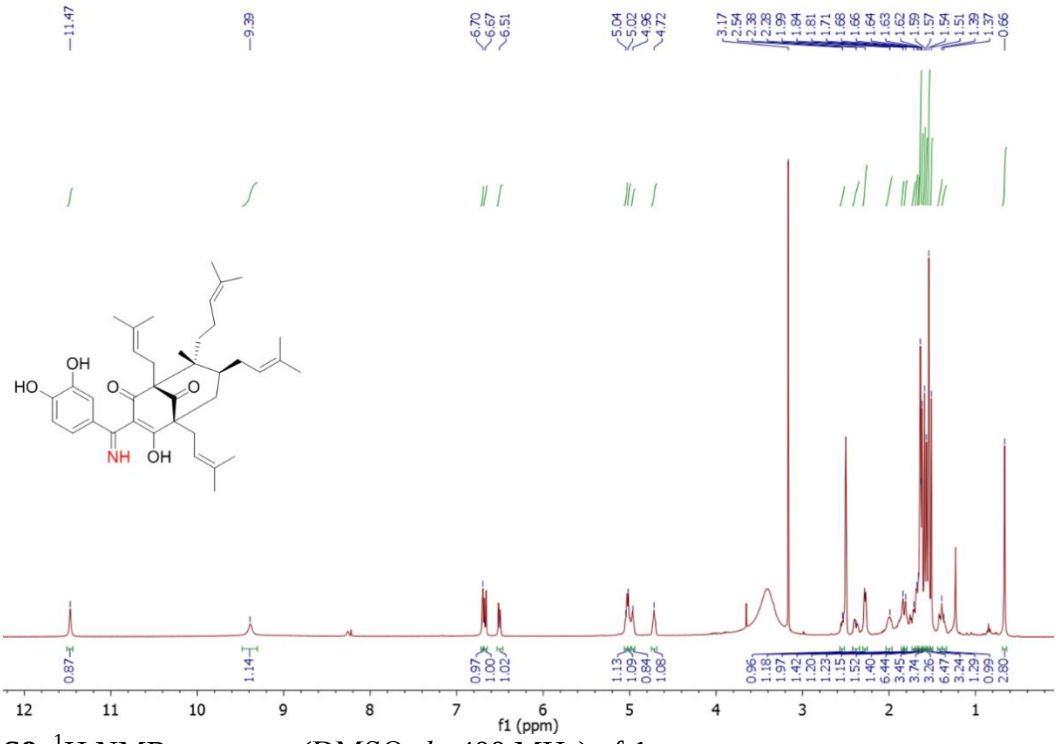

Figure S8. ^{1}H NMR spectrum (DMSO-d_6, 400 MH$_Z$) of **1**

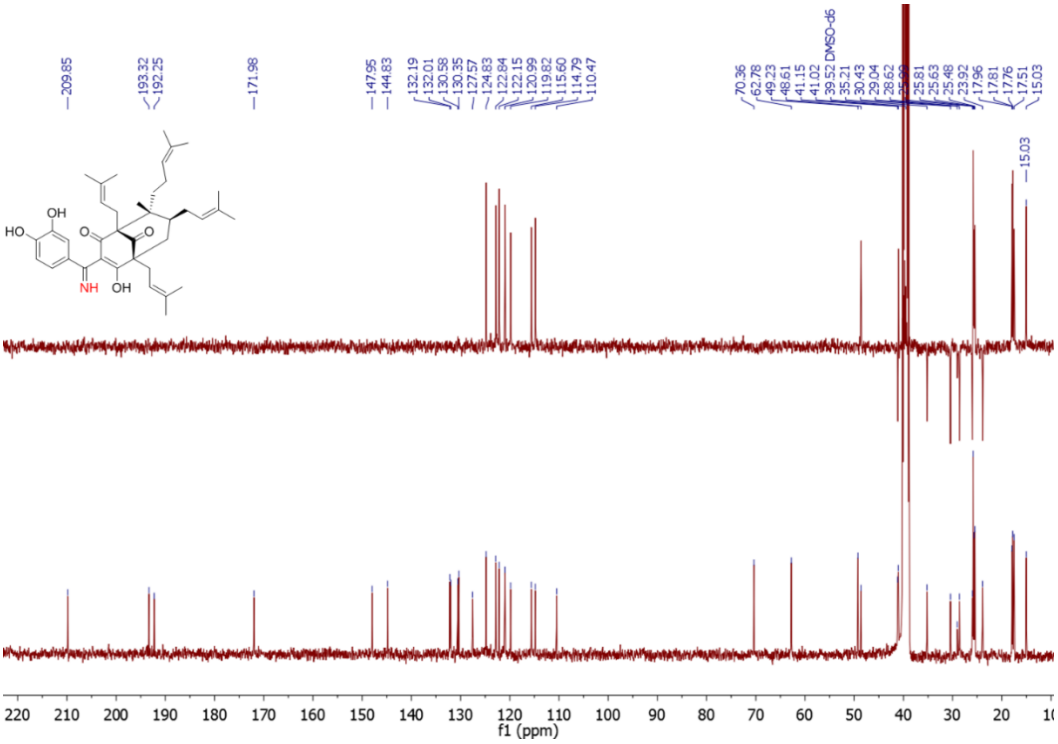

Figure S9. ^{13}C NMR and DEPT-135 spectra (DMSO-d_6, 100 MHz)of **1**

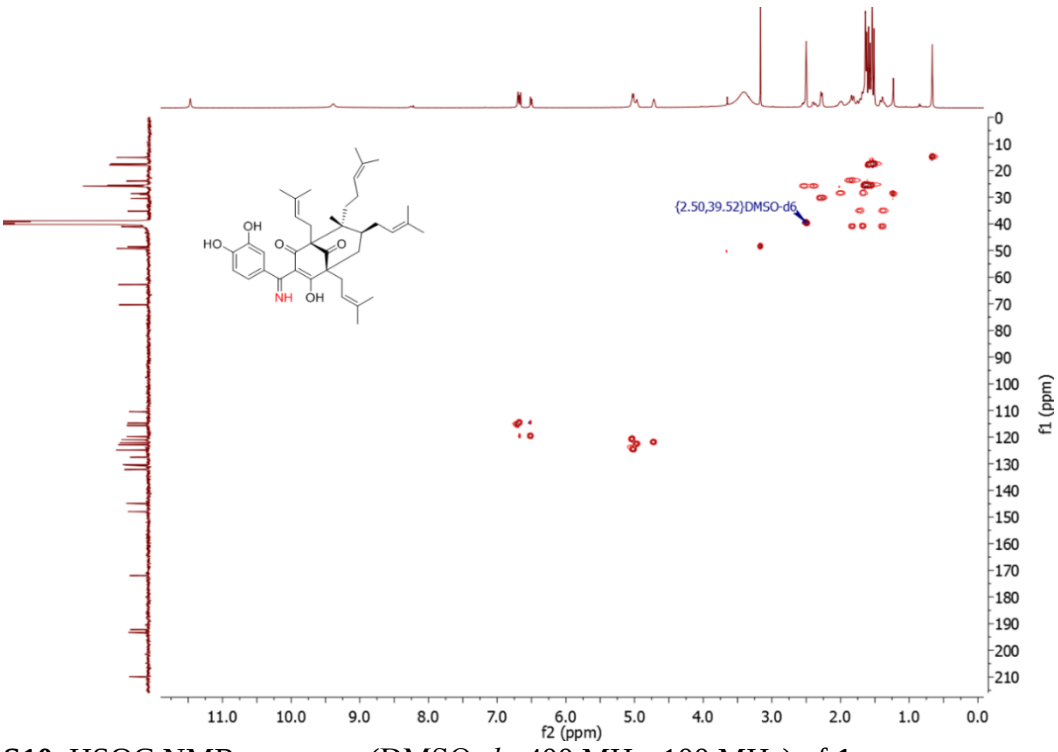

Figure S10. HSQC NMR spectrum (DMSO-d_6, 400 MHz, 100 MHz) of **1**

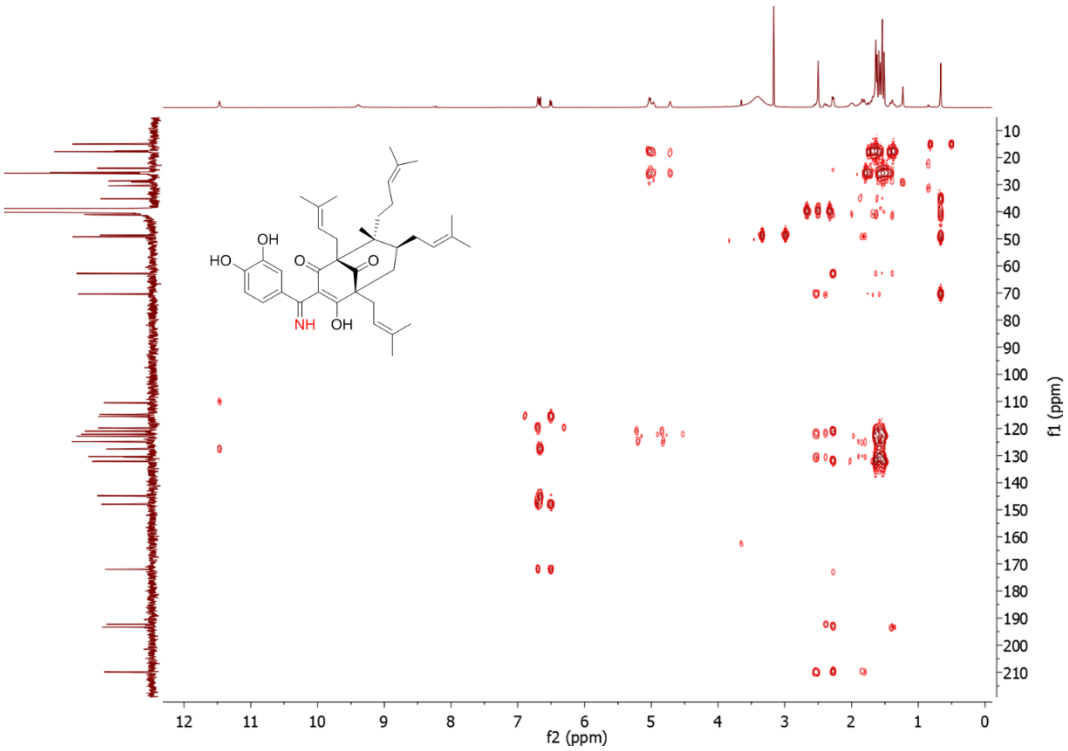

Figure S11. HMBC NMR spectrum (DMSO-d_6, 400 MH_Z, 100 MH_Z) of **1**

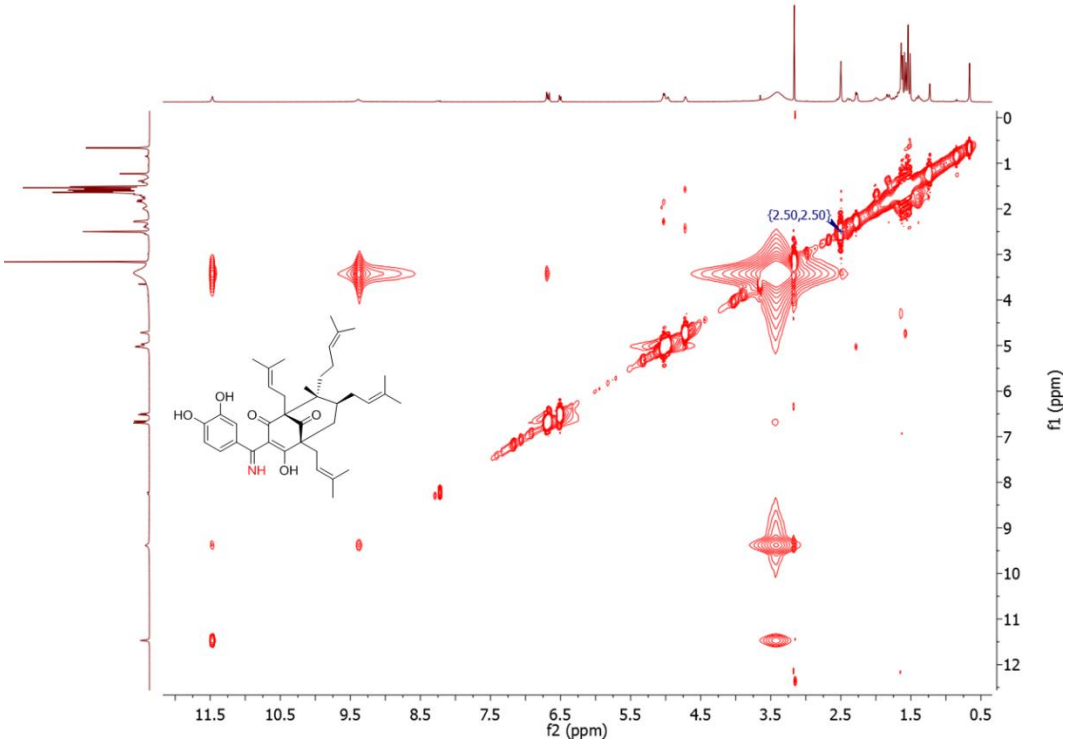

Figure S12. NOESY NMR spectrum (DMSO-d_6, 600 MH_Z, 150 MH_Z) of **1**

Garciyunnanimine B (**2**)

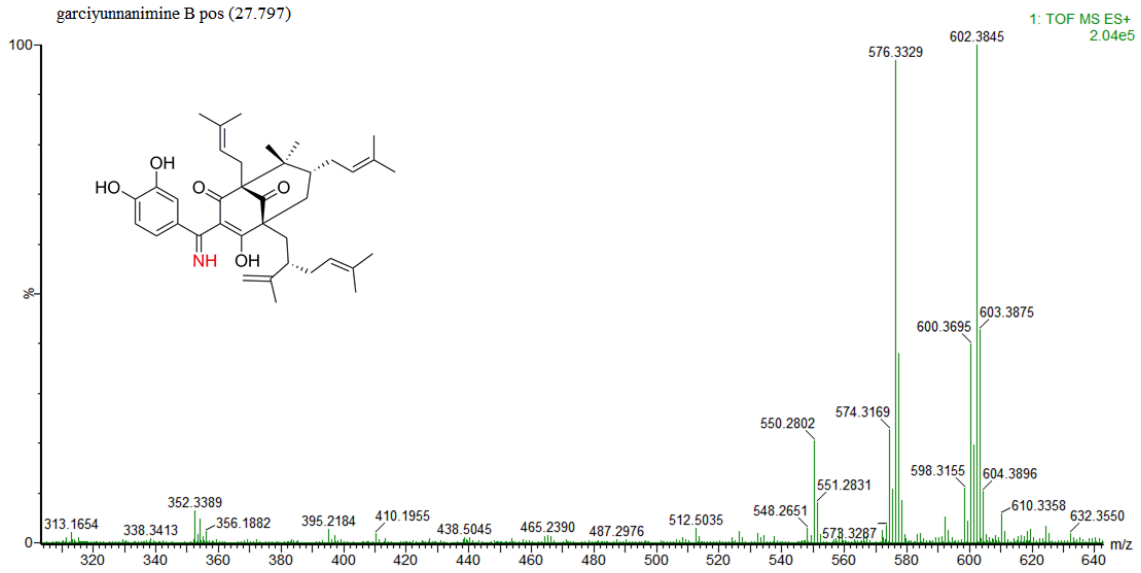

Figure S13. HRESIMS spectrum of **2**

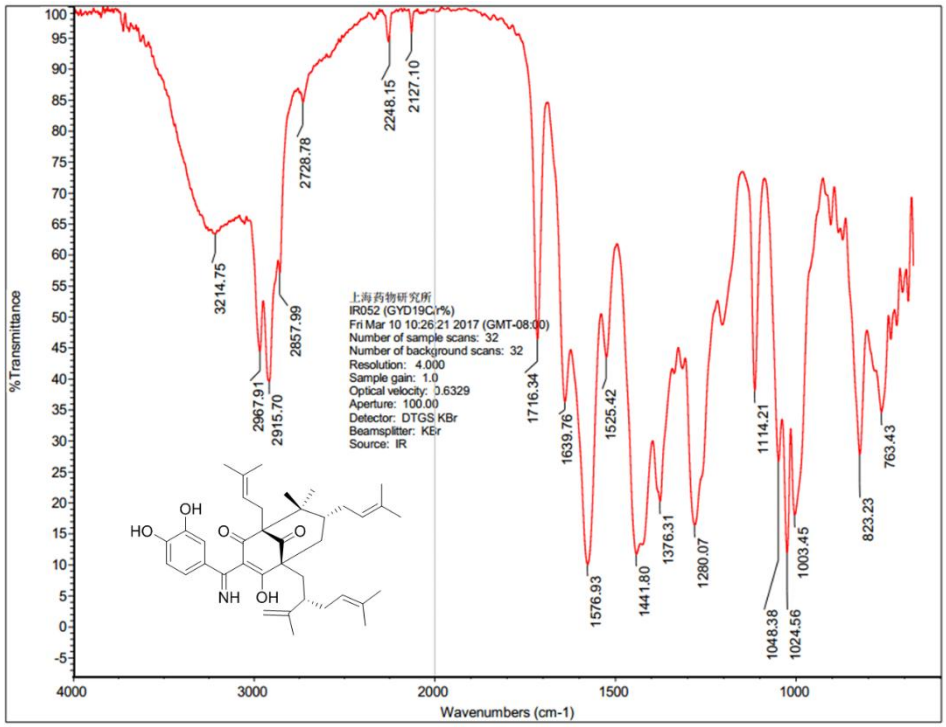

Figure S14. IR (KBr, disc) spectrum of **2**

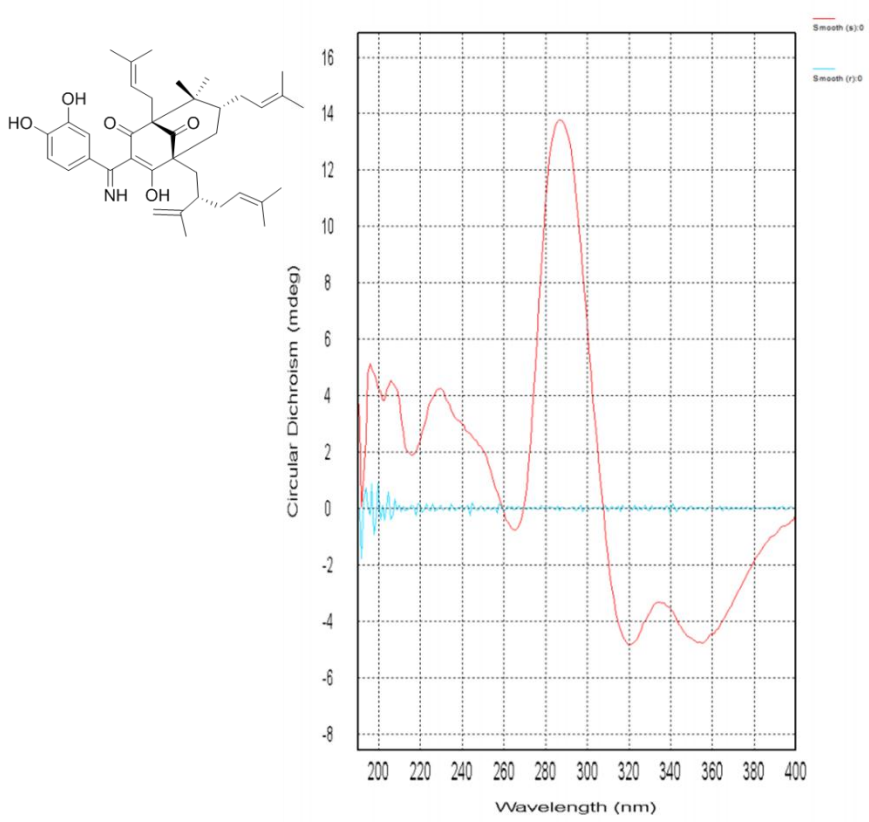

Figure S15. Experimental ECD spectrum of **2**

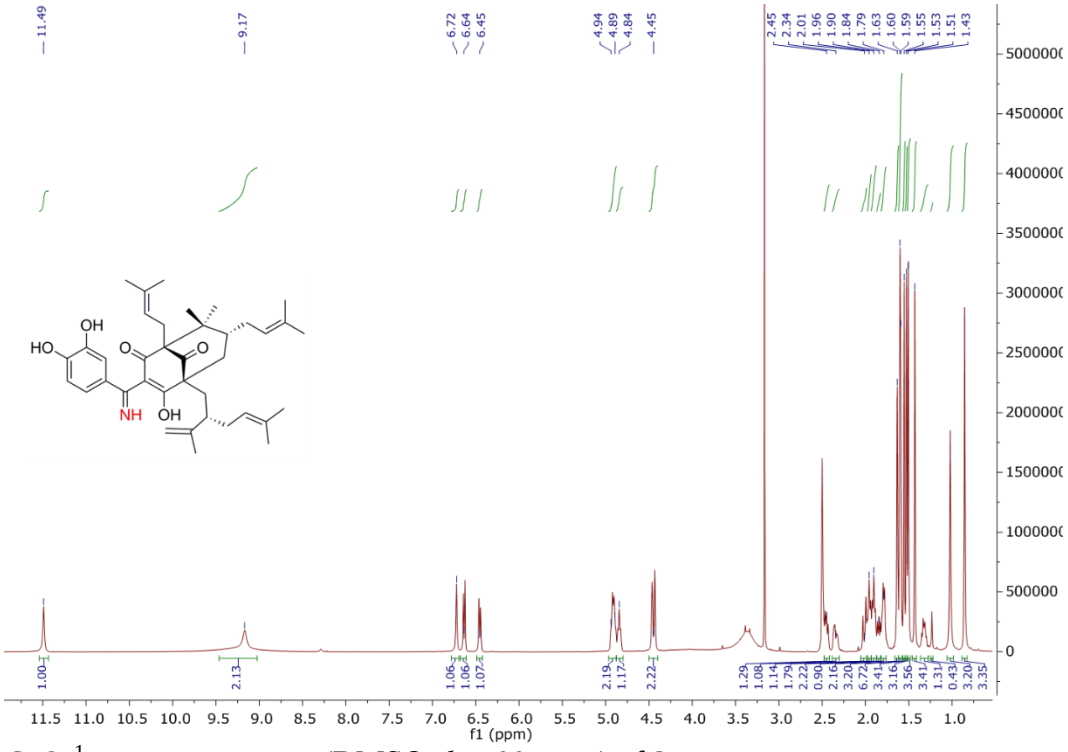

Figure S16. ^{1}H NMR spectrum (DMSO-d_6, 400 MH$_Z$) of **2**

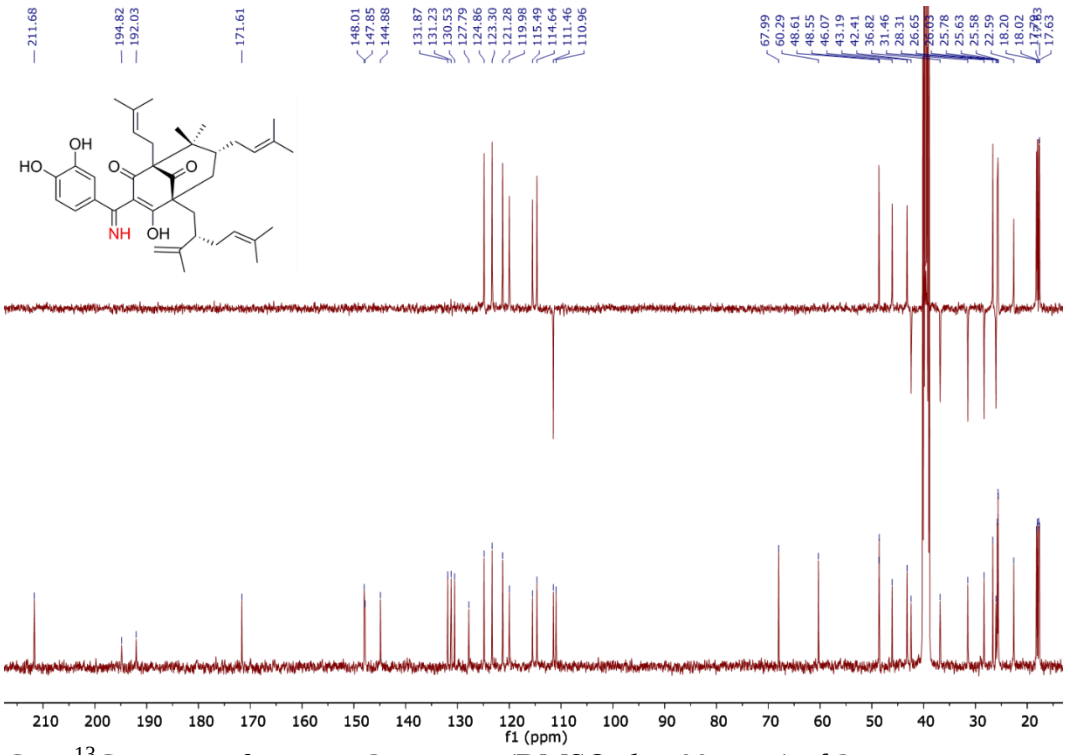

Figure S17. ^{13}C NMR and DEPT-135 spectra (DMSO-d_6, 100 MH$_Z$) of **2**

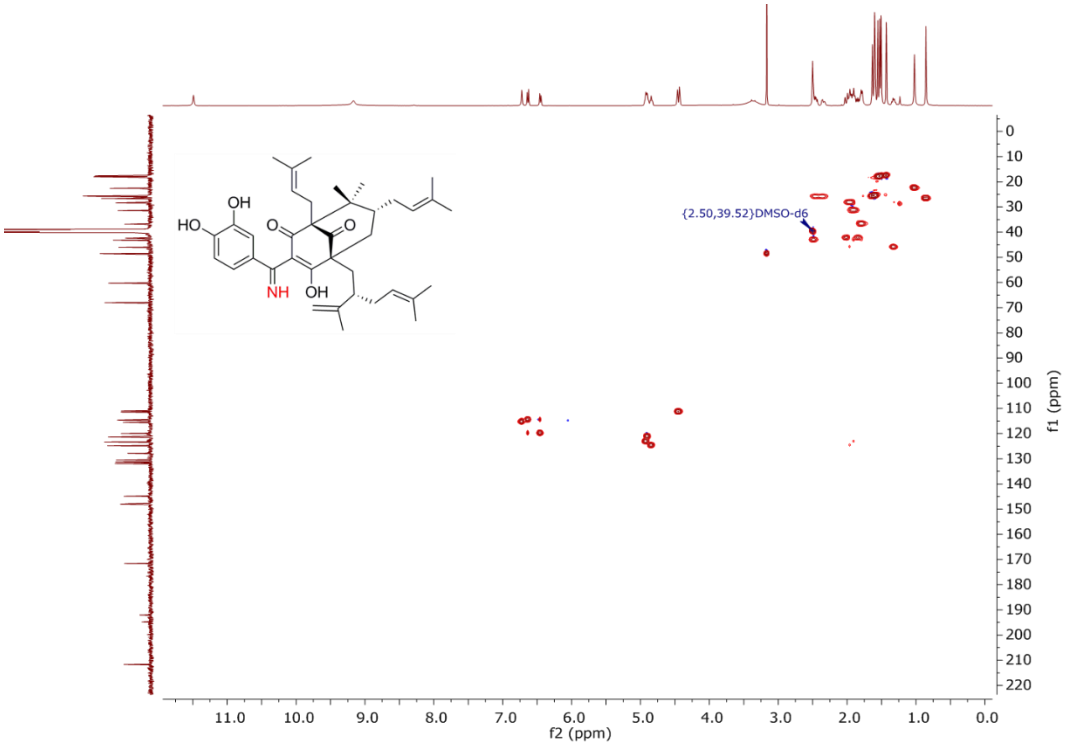

Figure S18. HSQC NMR spectrum (DMSO-d_6, 400 MH$_Z$, 100 MH$_Z$) of **2**

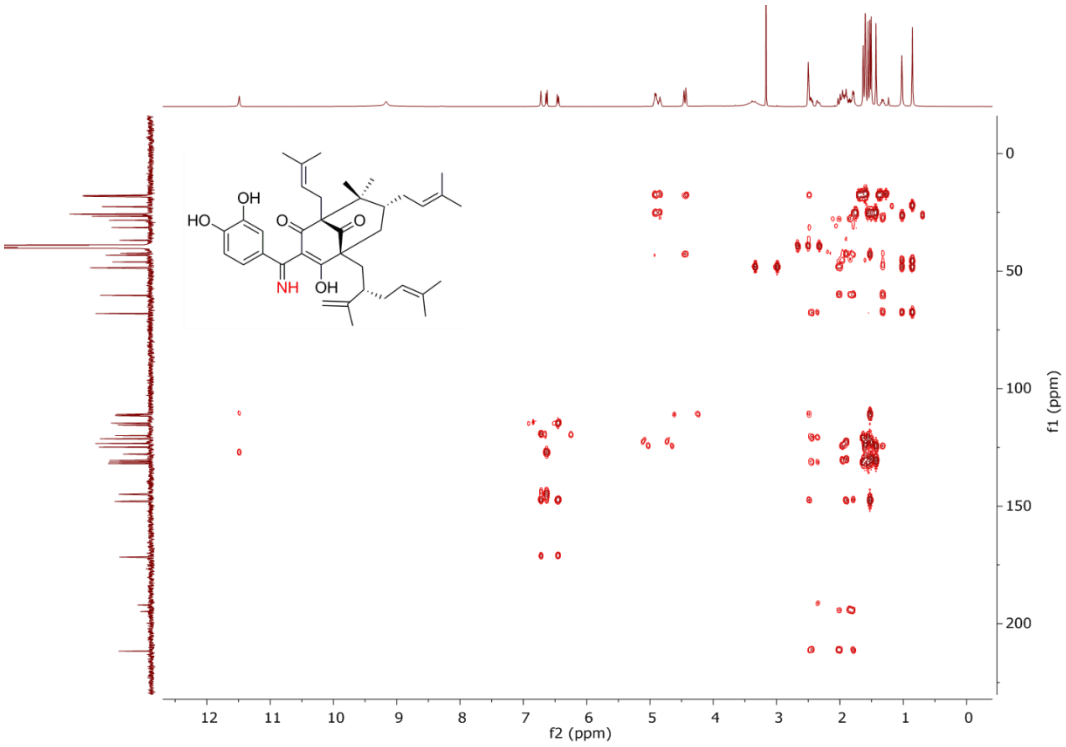

Figure S19. HMBC NMR spectrum (DMSO-d_6, 400 MH$_Z$, 100 MH$_Z$) of **2**

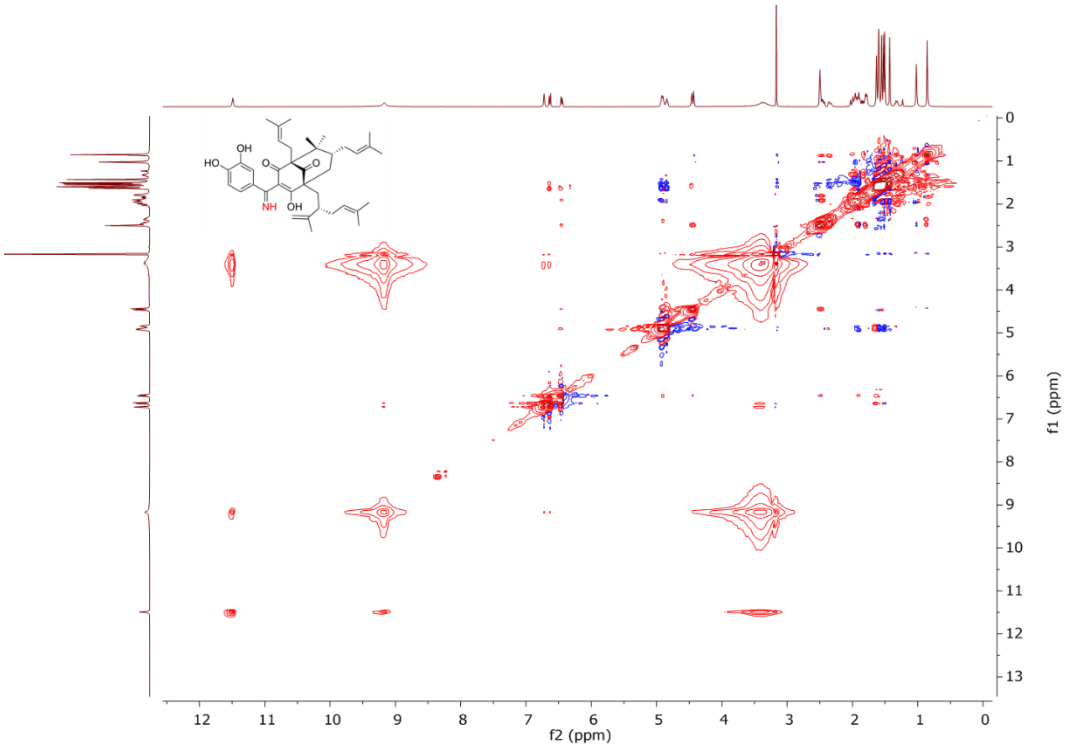

Figure S20. NOESY NMR spectrum (DMSO-d_6, 400 MH$_Z$, 100 MH$_Z$) of **2**

Garciyunnanimine C (**3**)

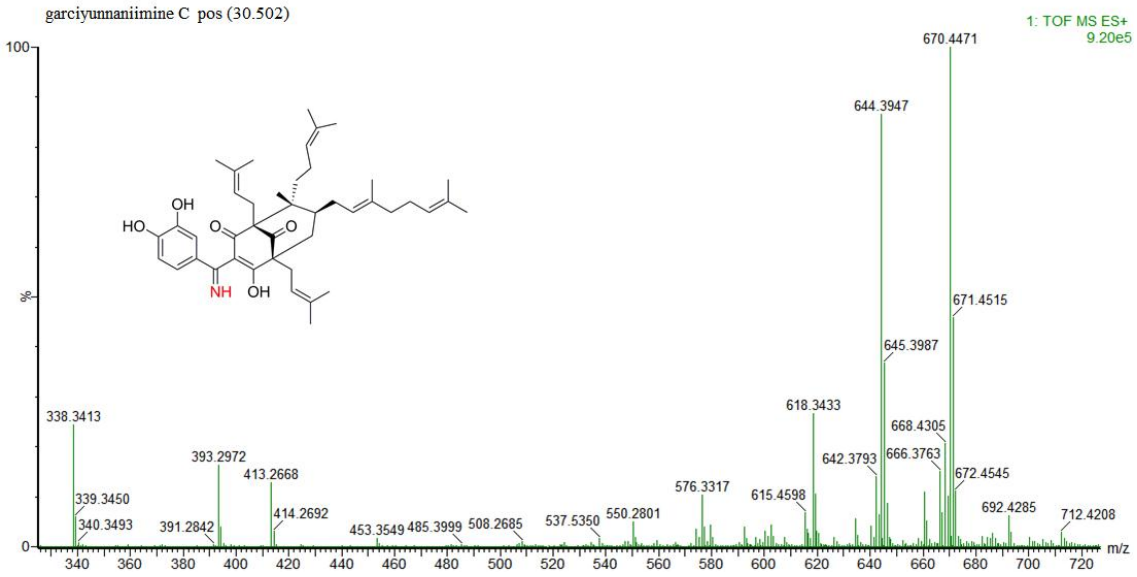

Figure S21. HRESIMS spectrum of **3**

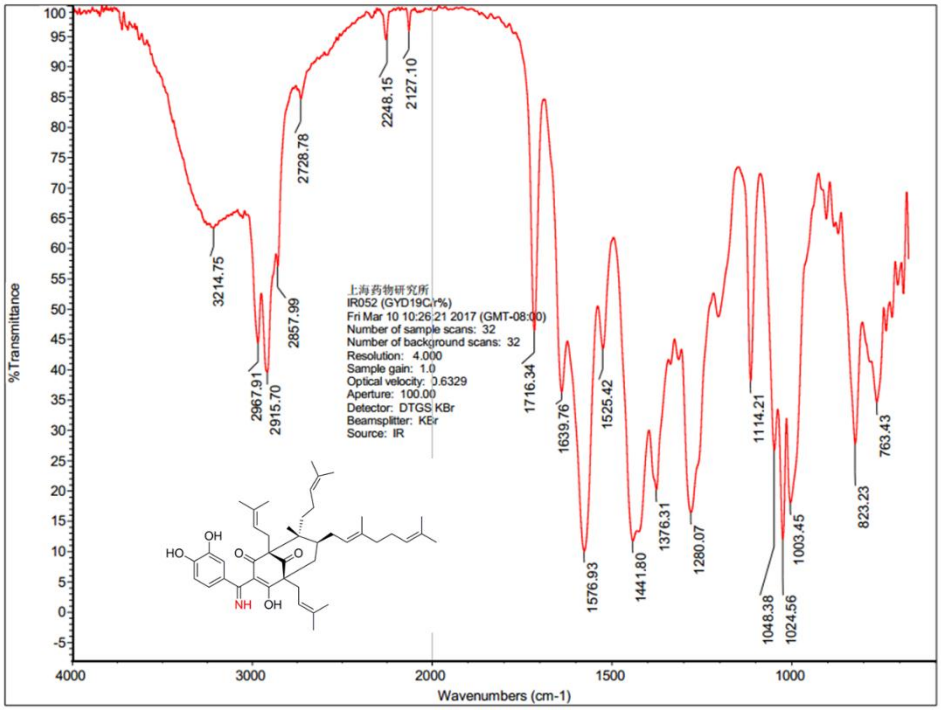

Figure S22. IR (KBr, disc) spectrum of **3**

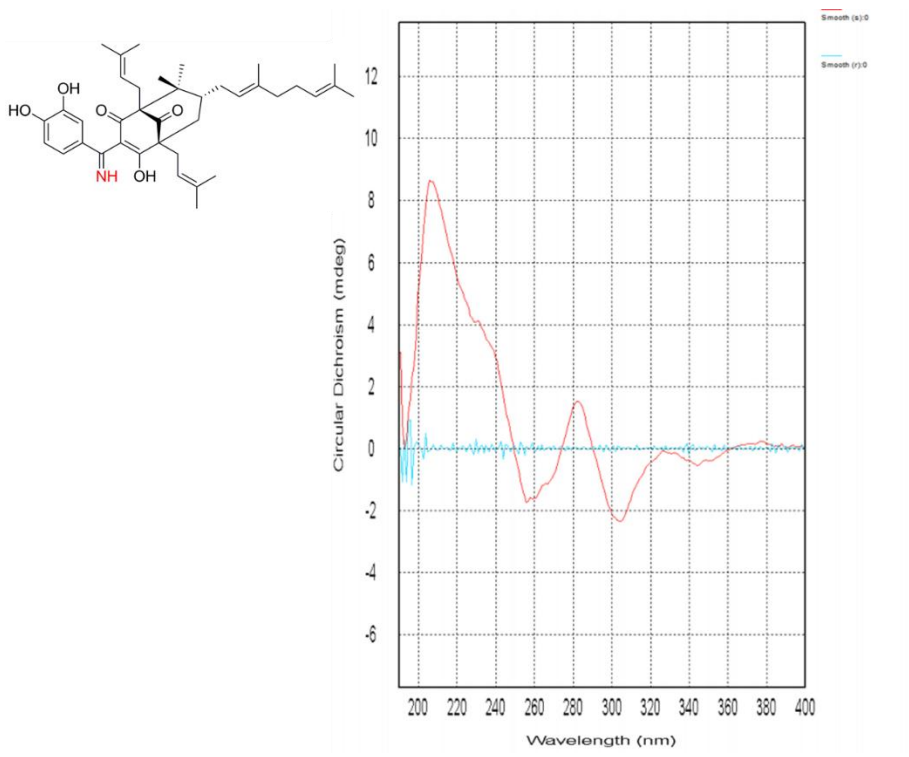

Figure S23. Experimental ECD spectrum of **3**

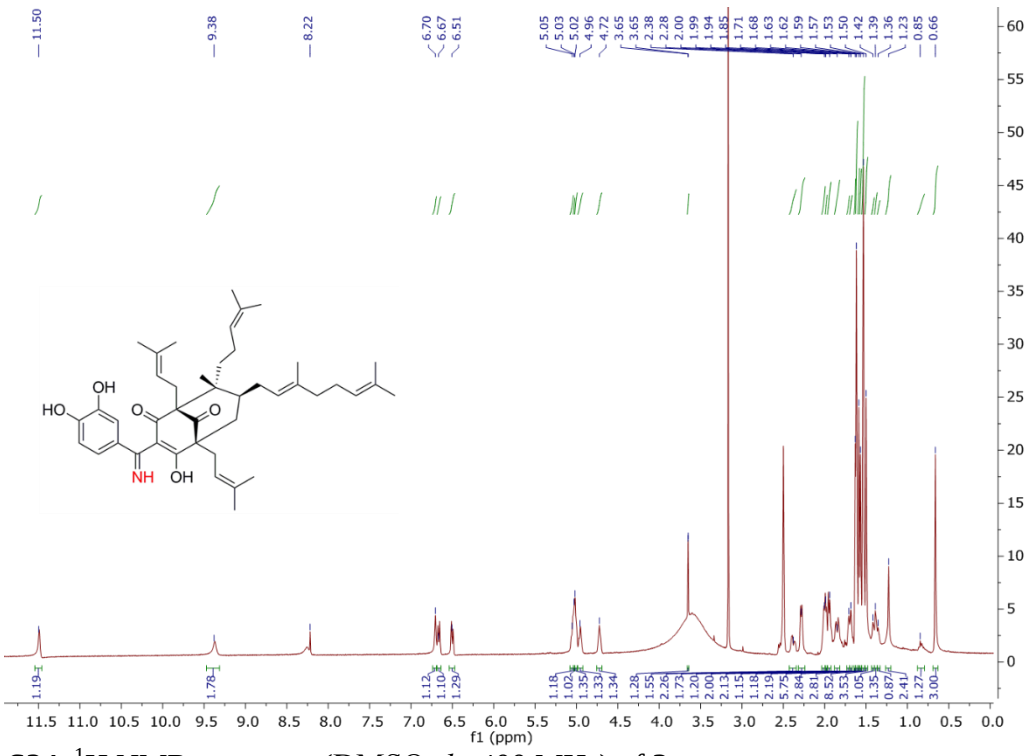

Figure S24. ^{1}H NMR spectrum (DMSO-d_6, 400 MH$_Z$) of **3**

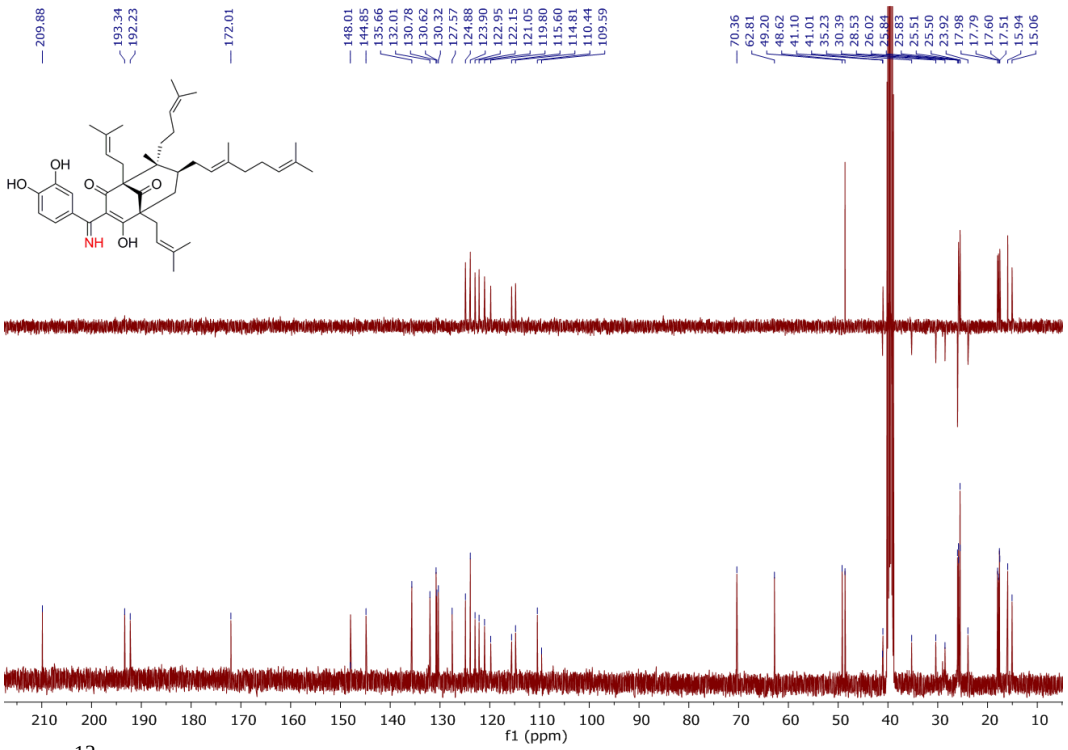

Figure S25. ^{13}C NMR and DEPT-135 spectra (DMSO-d_6, 100 MH$_Z$) of **3**

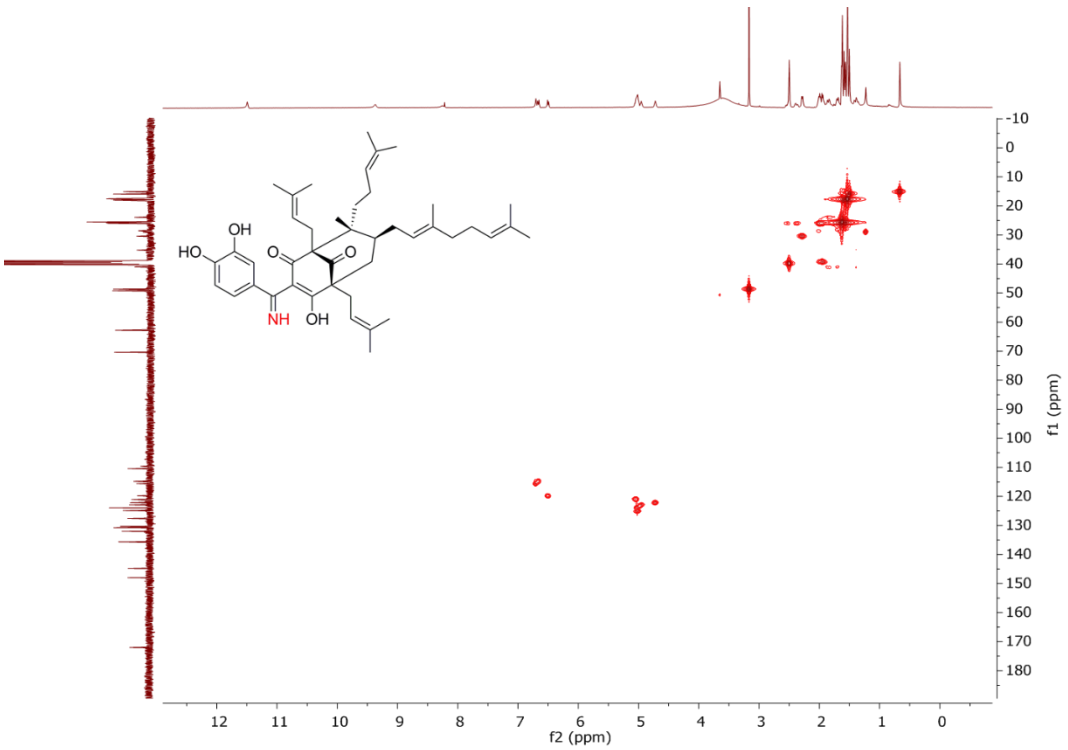

Figure S26. HSQC NMR spectrum (DMSO-d_6, 400 MH$_Z$, 100 MH$_Z$) of **3**

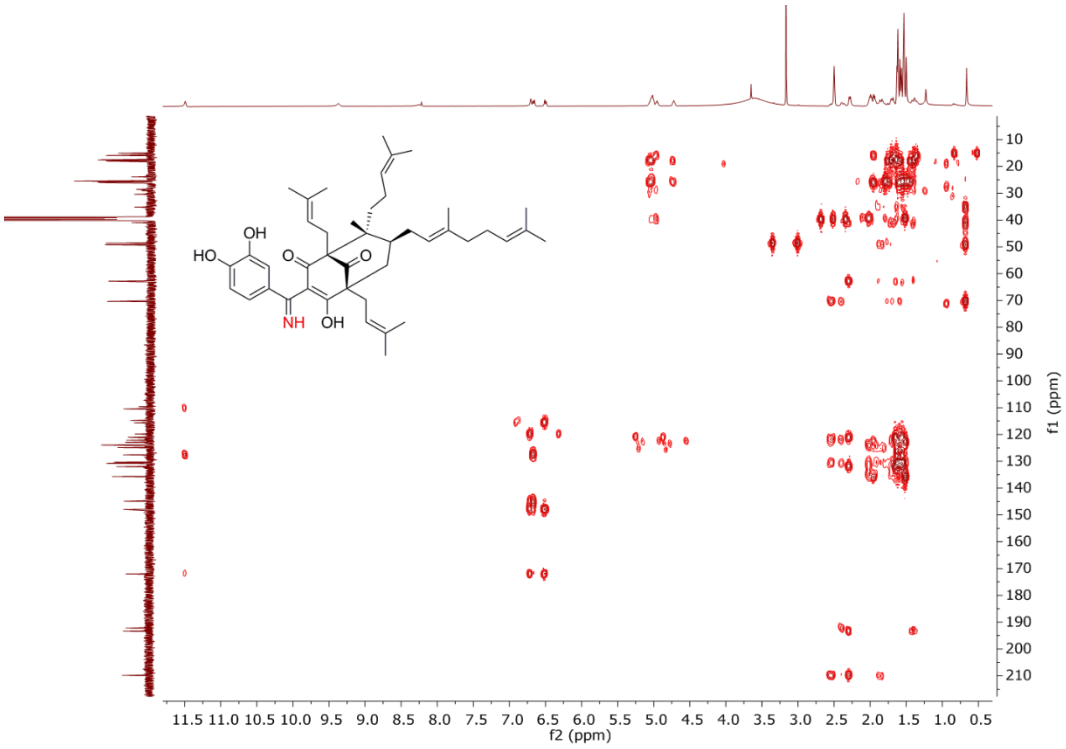

Figure S27. HMBC NMR spectrum (DMSO-d_6, 400 MHz, 100 MHz) of **3**

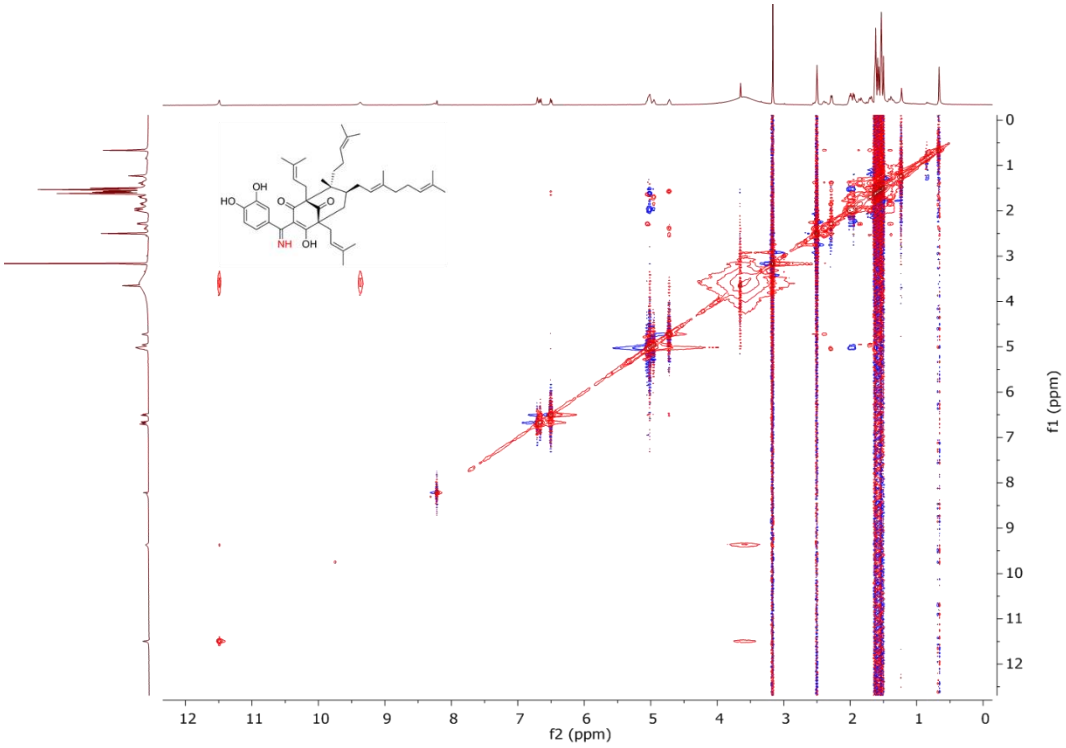

Figure S28. NOESY NMR spectrum (DMSO-d_6, 400 MHz, 100 MHz) of **3**

Garciyunnanimine D (**4**)

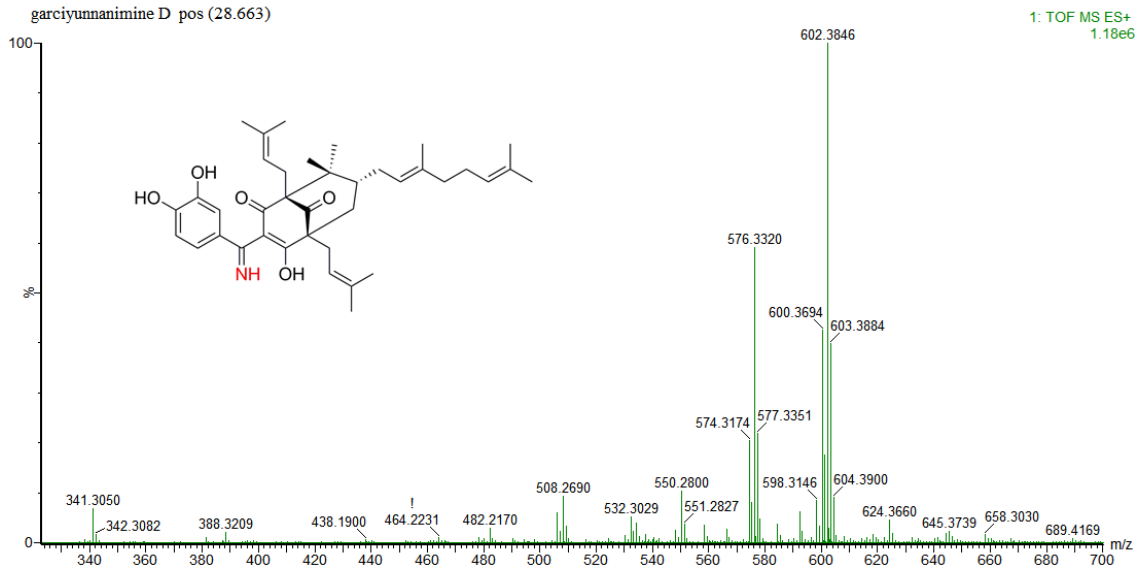

Figure S29. HRESIMS spectrum of **4**

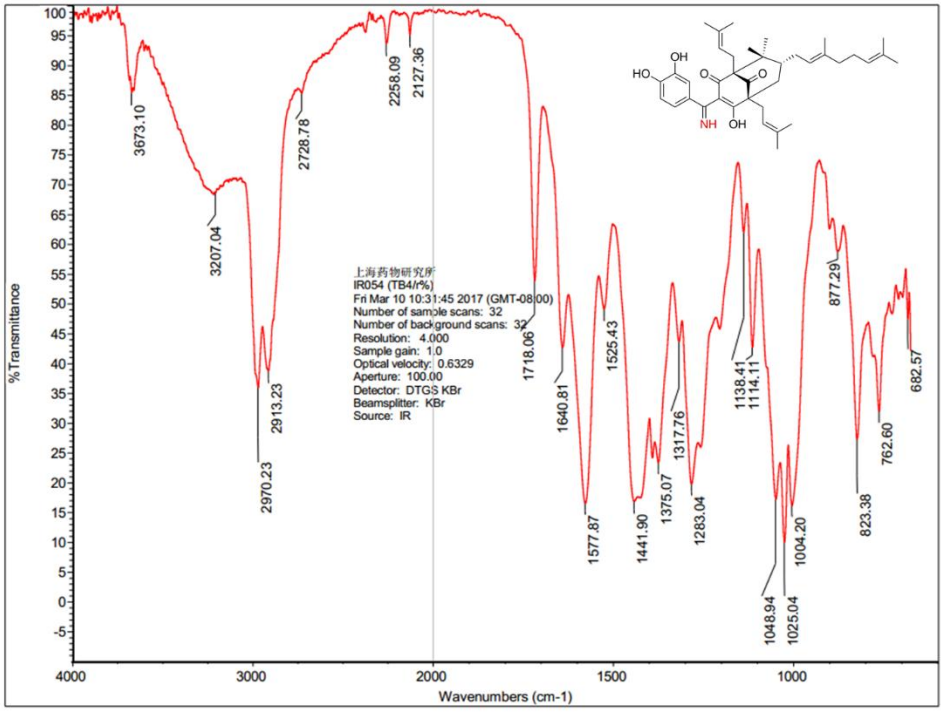

Figure S30. IR (KBr, disc) spectrum of **4**

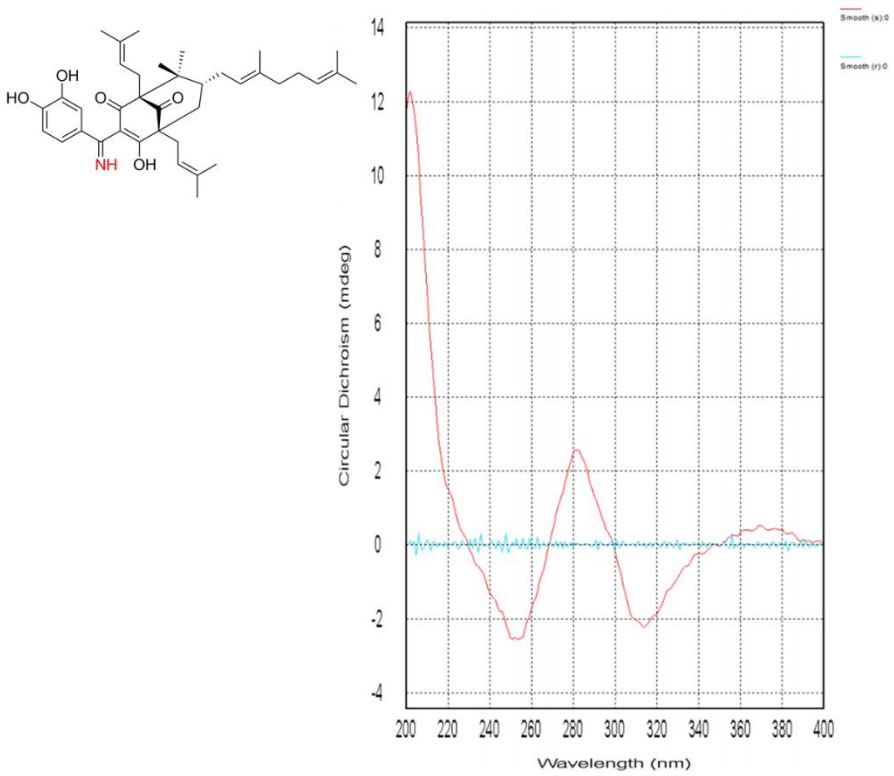

Figure S31. Experimental ECD spectrum of **4**

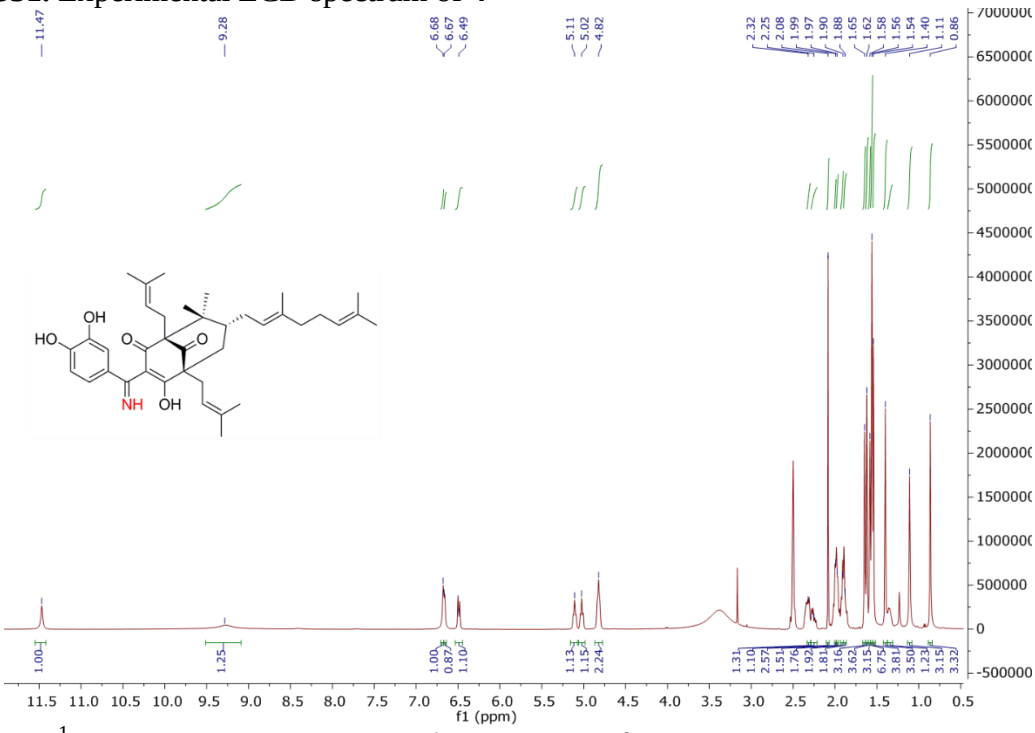

Figure S32. ^{1}H NMR spectrum (DMSO-d_6, 400 MH$_Z$) of **4**

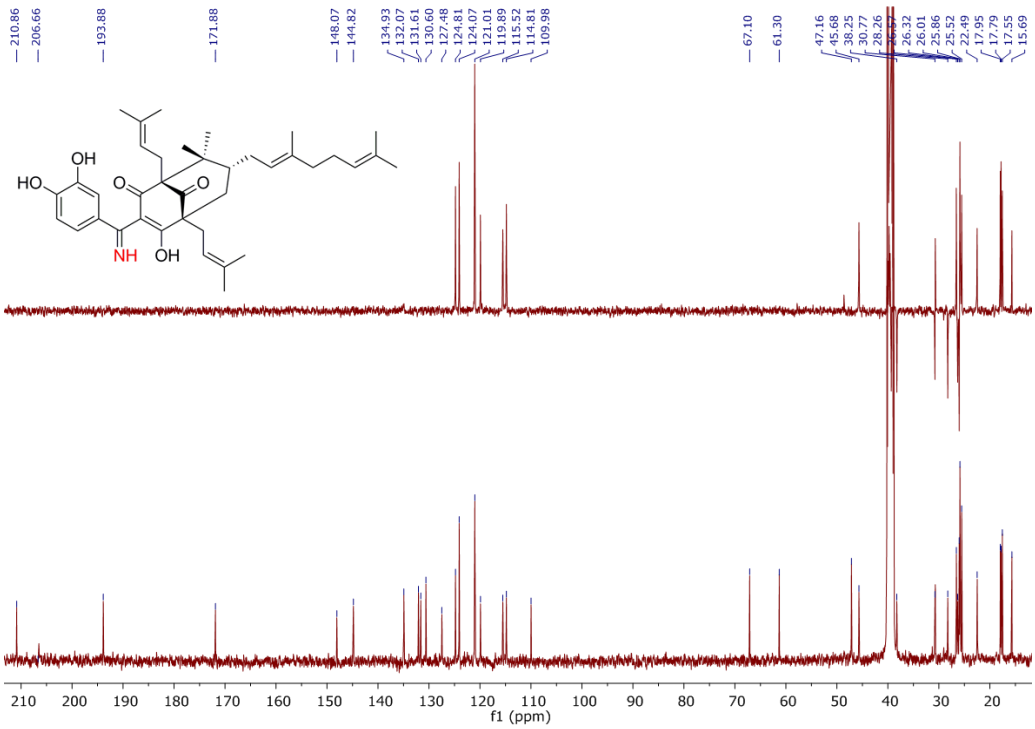

Figure S33. ^{13}C NMR and DEPT-135 spectra (DMSO-d_6, 100 MHz) of **4**

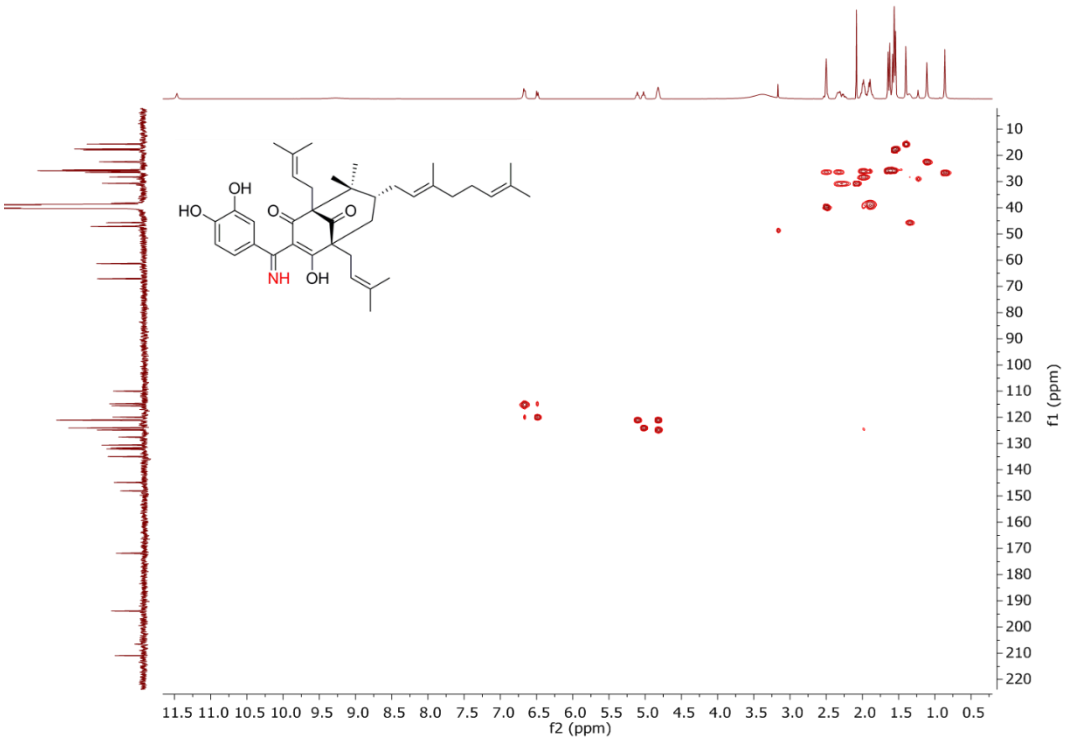

Figure S34. HSQC NMR spectrum (DMSO-d_6, 400 MHz, 100 MHz) of **4**

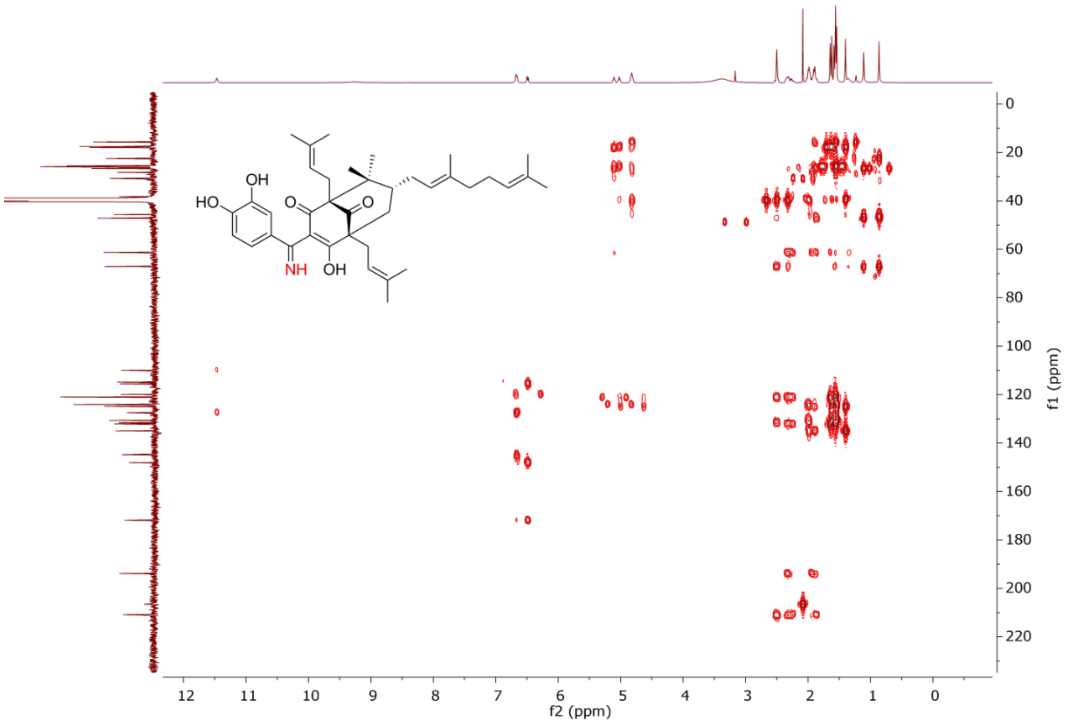

Figure S35. HMBC NMR spectrum (DMSO-d_6, 400 MH$_Z$, 100 MH$_Z$) of **4**

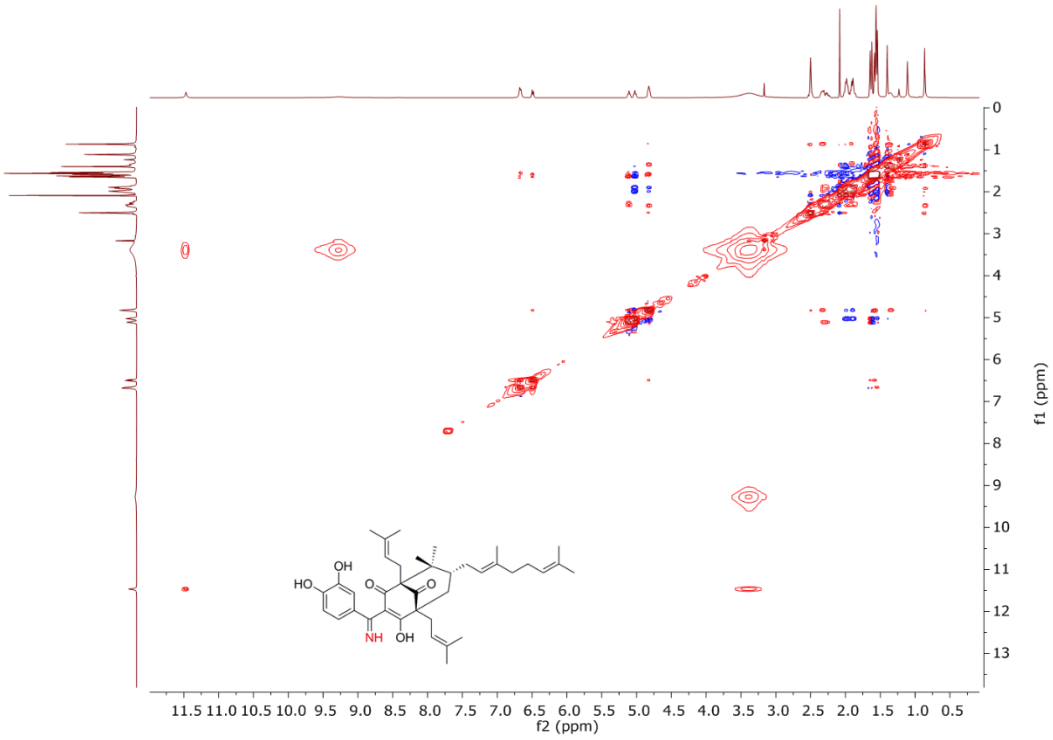

Figure S36. NOESY NMR spectrum (DMSO-d_6, 400 MH$_Z$, 100 MH$_Z$) of **4**

Garciyunnanimine E (**5**)

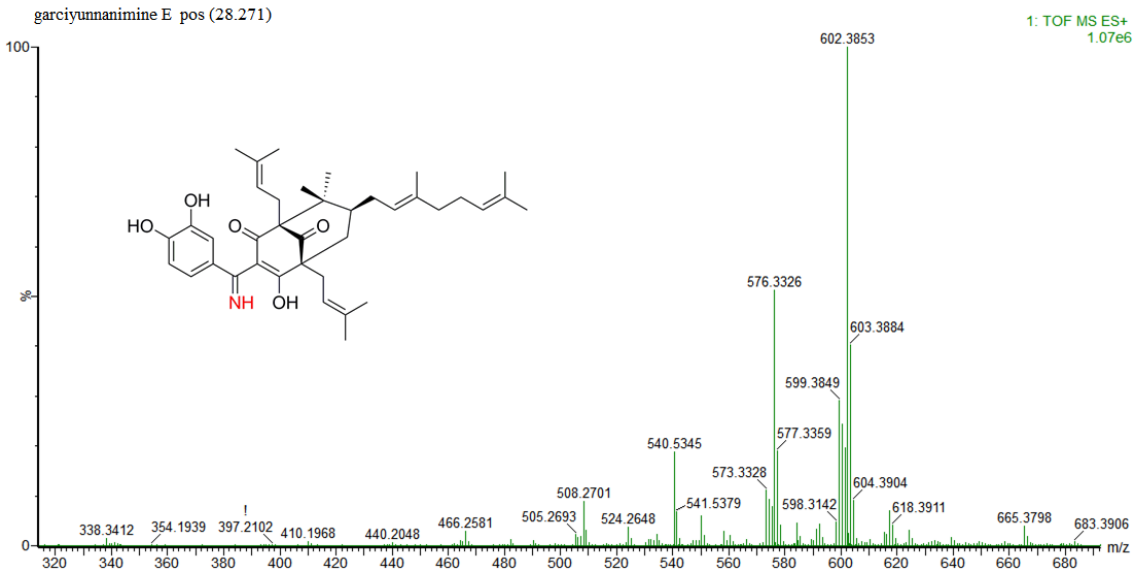

Figure S37. HRESIMS spectrum of **5**

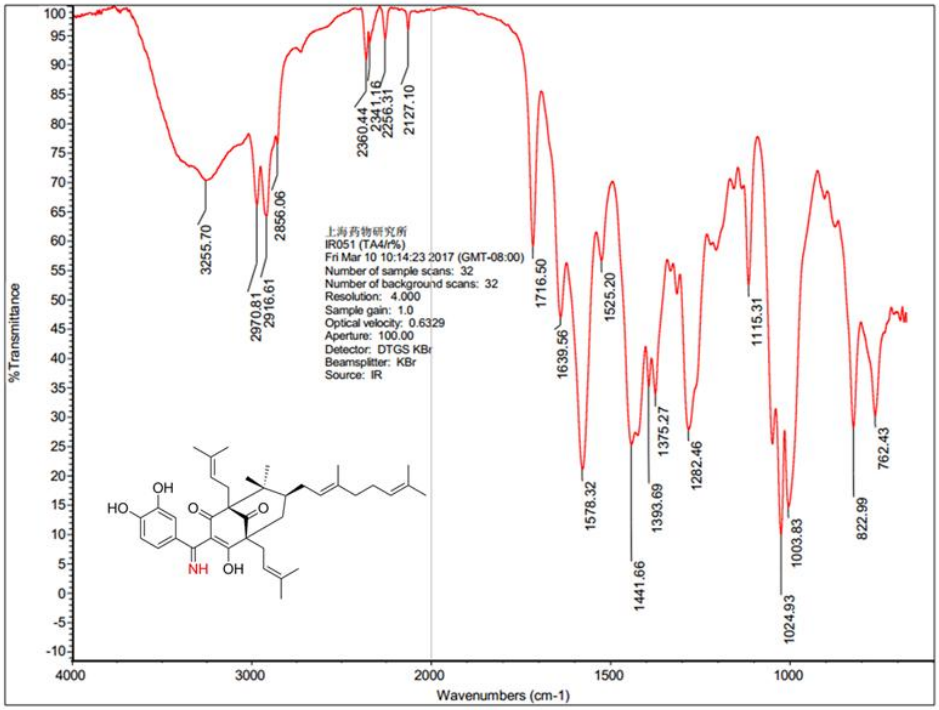

Figure S38. IR (KBr, disc) spectrum of **5**

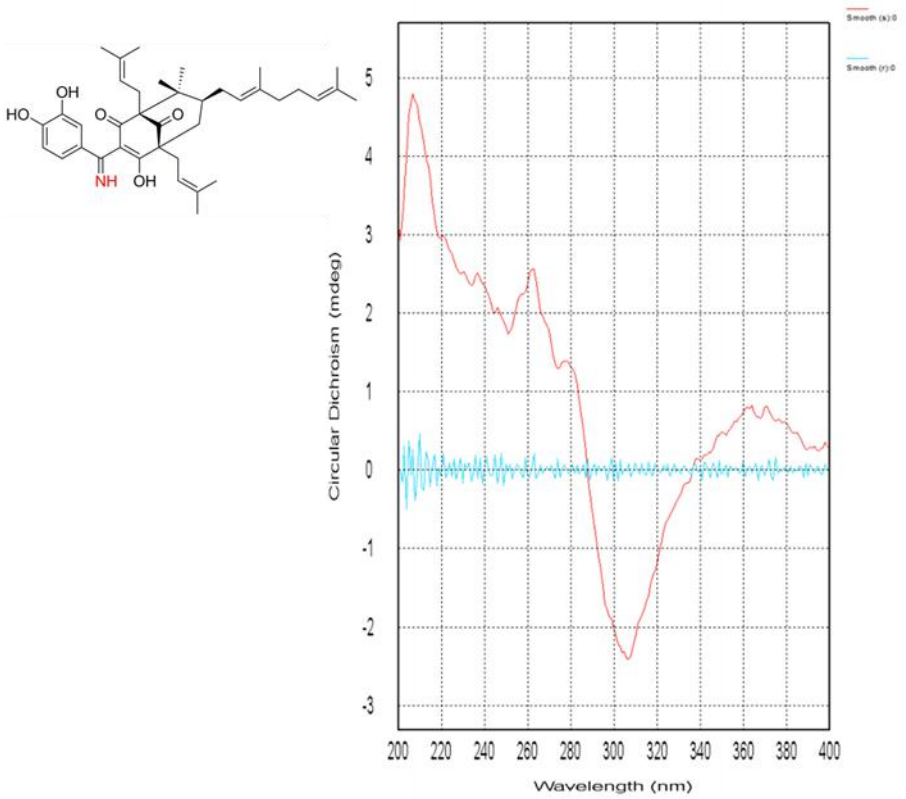

Figure S39. Experimental ECD spectrum of **5**

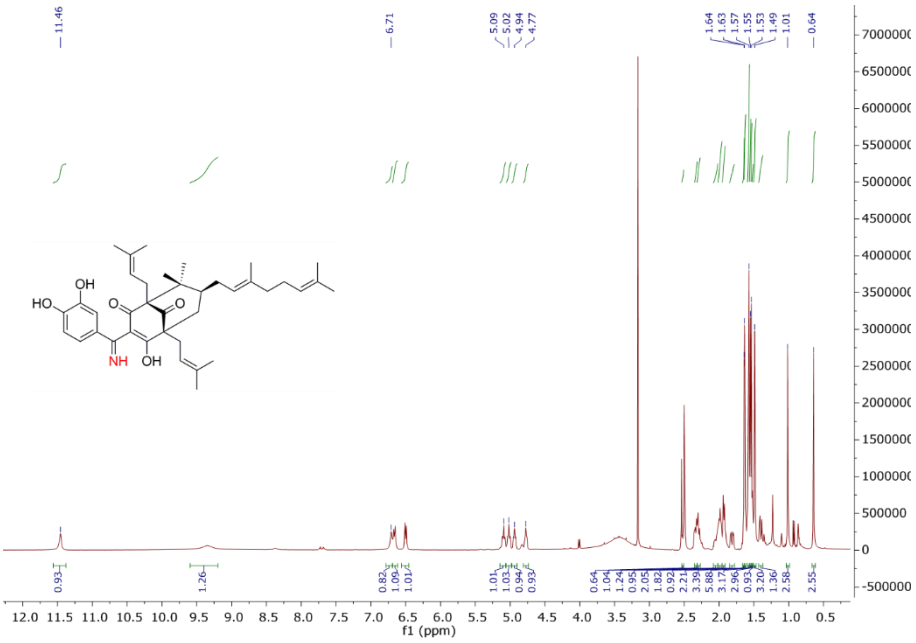

Figure S40. ^{1}H NMR spectrum (DMSO-d_6, 400 MH$_Z$) of **5**

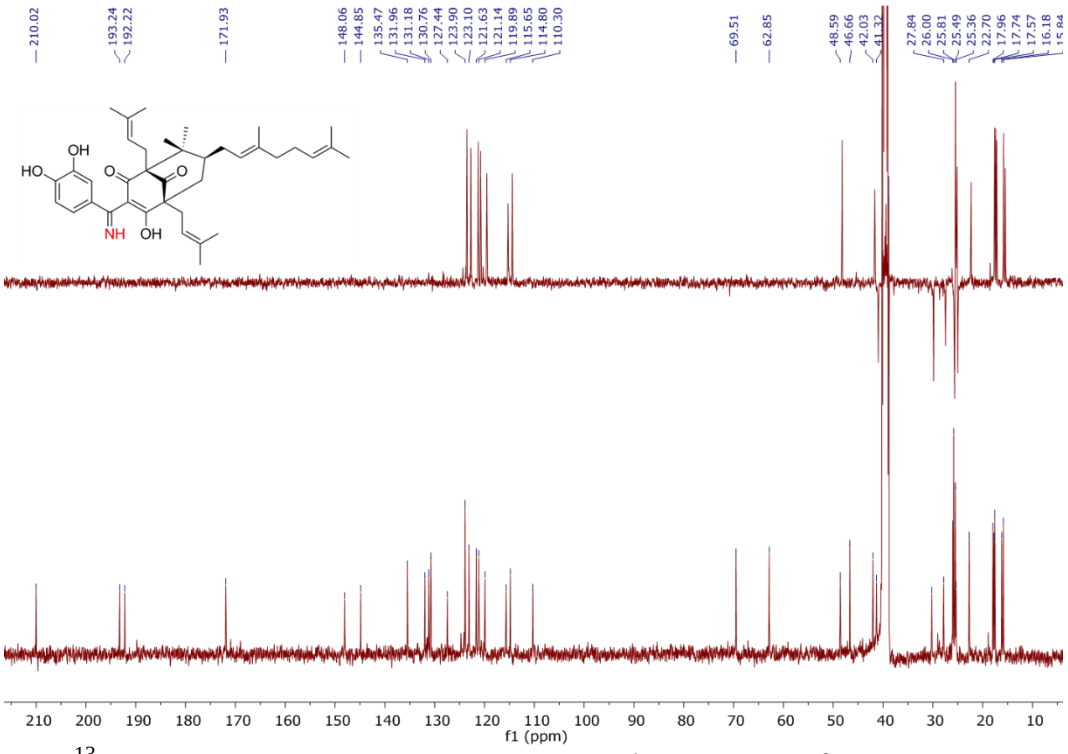

Figure S41. ^{13}C NMR and DEPT-135 spectra (DMSO-d_6, 100 MHz) of **5**

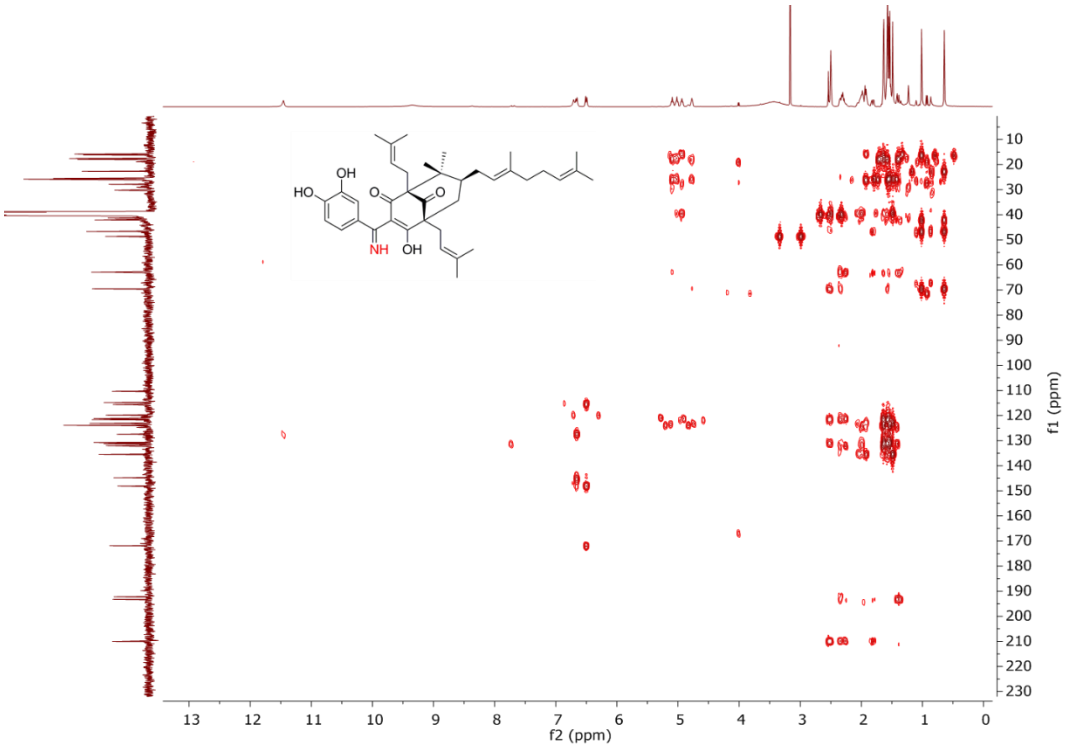

Figure S42. HSQC NMR spectrum (DMSO-d_6, 400 MHz, 100 MHz) of **5**

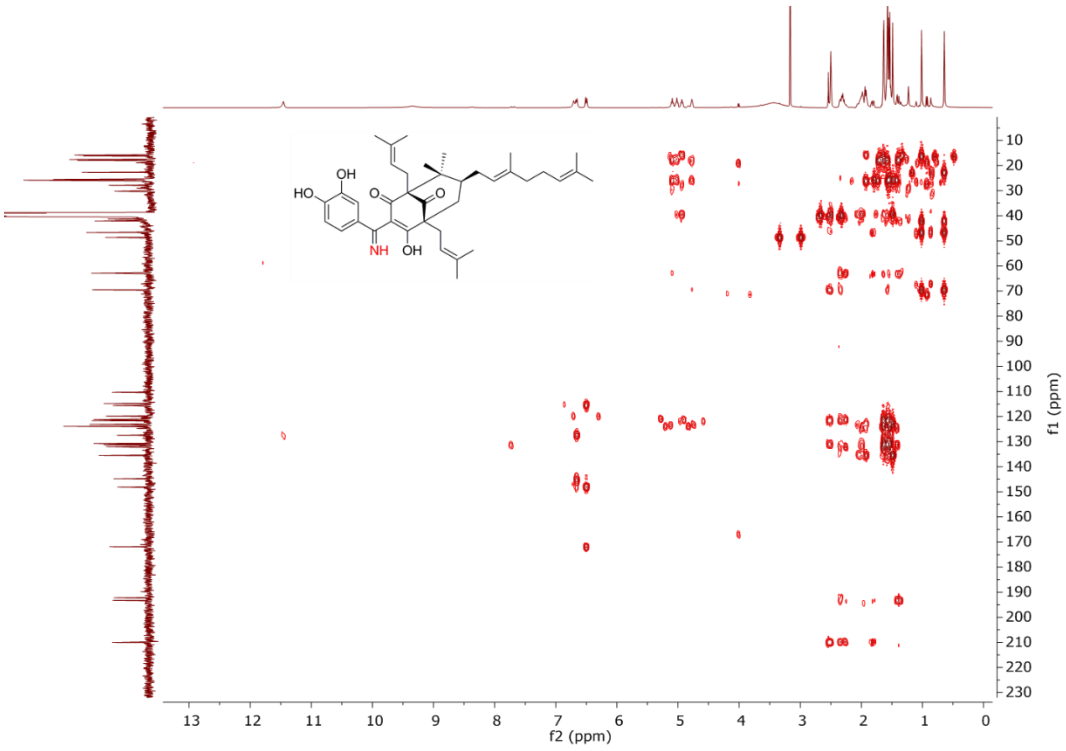

Figure S43. HMBC NMR spectrum (DMSO-d_6, 400 MH_Z, 100 MH_Z) of **5**

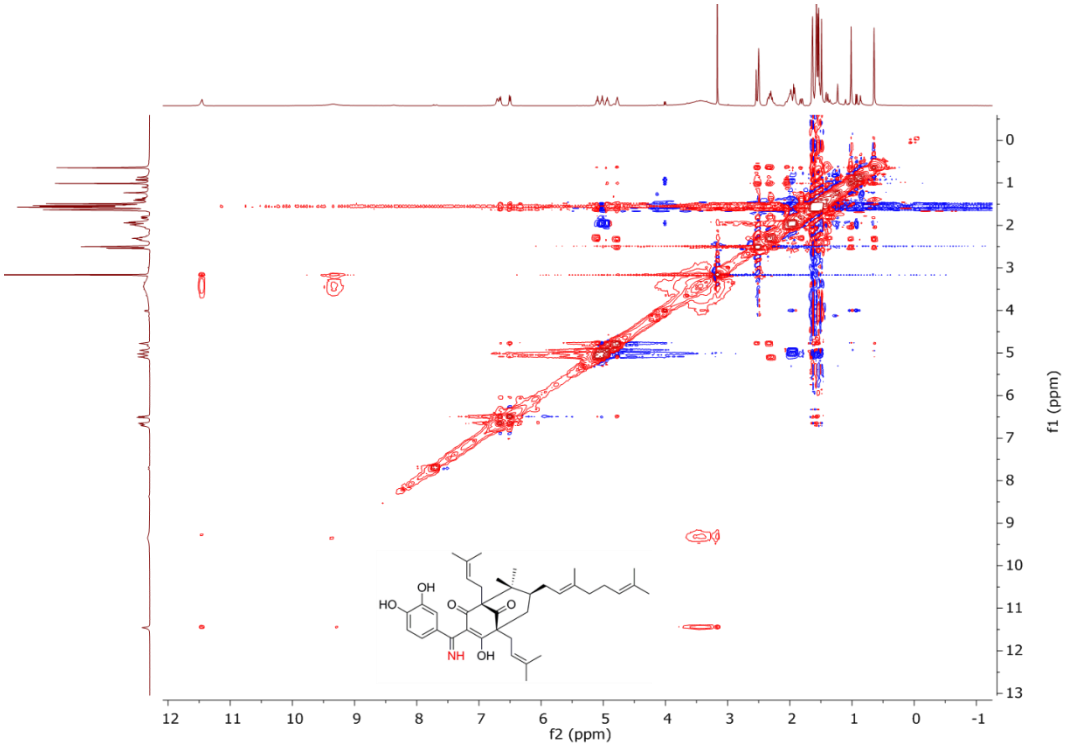

Figure S44. NOESY NMR spectrum (DMSO-d_6, 400 MH_Z, 100 MH_Z) of **5**